



HAL
open science

A Deformed Wedge-Top Basin Inverted During the Collapse of the Variscan Belt: The Permo-Carboniferous Lorraine Basin (NE France)

R. Hemelsdaël, Olivier Averbuch, Laurent Beccaletto, A. Izart, Stéphane Marc, Laure Capar, R. Michels

► To cite this version:

R. Hemelsdaël, Olivier Averbuch, Laurent Beccaletto, A. Izart, Stéphane Marc, et al.. A Deformed Wedge-Top Basin Inverted During the Collapse of the Variscan Belt: The Permo-Carboniferous Lorraine Basin (NE France). *Tectonics*, 2023, 42 (11), pp.1-27. 10.1029/2022TC007668. hal-04285167v2

HAL Id: hal-04285167

<https://hal.science/hal-04285167v2>

Submitted on 1 Feb 2024

HAL is a multi-disciplinary open access archive for the deposit and dissemination of scientific research documents, whether they are published or not. The documents may come from teaching and research institutions in France or abroad, or from public or private research centers.

L'archive ouverte pluridisciplinaire **HAL**, est destinée au dépôt et à la diffusion de documents scientifiques de niveau recherche, publiés ou non, émanant des établissements d'enseignement et de recherche français ou étrangers, des laboratoires publics ou privés.

A Deformed Wedge-Top Basin Inverted During the Collapse of the Variscan Belt: The Permo-Carboniferous Lorraine Basin (NE France)

Romain Hemelsdaël^{1*}, Olivier Averbuch², Laurent Beccaletto³, Alain Izart⁴, Stéphane Marc³, Laure Capar³, Raymond Michels¹

Abstract

A new structural model is presented for the Permo-Carboniferous Lorraine Basin (NE France), a major intramountain basin that developed during the latest stages of the Variscan orogeny (ca. 315–270 Ma). Digitalized well logs and reprocessed seismic data were used to decipher the kinematic evolution of this basin located along the Rhenohercynian orogenic suture zone. The basin was initiated during the late collision stage (Early to Middle Pennsylvanian) in a wedge-top position upon the Saxothuringian retro-wedge. The syn-orogenic sequence is delimited to the north by the major SE-verging Metz Thrust, which is part of the backthrust system that propagated during Middle Pennsylvanian (Late Westphalian). Seismic data provide evidence of negative tectonic inversion, allowing the formation of synrift depocenters (Late Pennsylvanian-Early Permian) above the former anticlines. Erosion of these anticlines results in a major unconformity marking the onset of post-orogenic collapse. The late Early Permian shortening (Saalian phase) is suggested to reactivate former thrusts and normal faults, thus generating late uplift of the basin. The post-orogenic phase is complex and diachronous at basin scale, and both compression and extension can be recorded in the same area over a short period (less than 10 Myr). The Late Carboniferous negative tectonic inversion along the Rhenohercynian suture zone is proposed to result from the lithospheric delamination of the Variscan orogenic roots. The associated upwelling of asthenospheric material is recorded by intense magmatic activity, and can be, in turn, considered as the main trigger for the subsequent thermal subsidence of the Mesozoic Paris Basin.

¹ *GéoRessources, Université de Lorraine, CNRS, UMR 7359, Vandœuvre-le s-Nancy, France*

² *LOG—Laboratoire d’Océanologie et de Géosciences, Université de Lille, CNRS, Université du Littoral Côte d’Opale, UMR 8187, Lille, France*

³ *BRGM, Orléans, France*

⁴ *202 Chemin de Cabanis, Prades-le-Lez, France*

***Corresponding author:** r.hemelsdael@gmail.com

Contents

1	Introduction	3	4.2	Evidence for the Syn-Orogenic Character of the Westphalian Unit	11
2	Geological Setting of the Lorraine-Saar-Nahe Basin (LSNB)	3	4.3	Negative Tectonic Inversion and Its Control on the Development of synrift Depocenters	11
2.1	Variscan Tectonic Framework	3	4.4	Transverse Faults	16
2.2	Structural Development of the LSNB	5	4.5	Local Reactivation During the Early Permian Saalian Compressive Phase	16
2.3	Stratigraphy of the LSNB	7	4.6	Geometry of the Basin Bounding Faults	16
3	Seismic and Well Data	8	5	A New Tectonic Model for the LSNB	18
3.1	Seismic Acquisitions and Reprocessing	8	5.1	Integration of Seismic Data Into a New Regional Structural Map	18
3.2	Seismic-Well Tie	9	5.2	Structural Development of the Permo-Carboniferous LSNB	20
4	Seismic Interpretations	9	6	Conclusions	22
4.1	Overview of the Main Seismic Features and Facies	9		Acknowledgments	23

1. Introduction

Since the late eighties, the late evolution of collisional orogenic systems and the return to post-orogenic gravitationally stable lithospheric conditions have been the focus of a large number of geodynamic studies. The main outcome of these studies is that the long-term destruction of the orogenic relief is not only achieved by denudation but also by tectonic collapse (Burg et al., 1994; Dewey, 1988; Malavieille et al., 1990; Ménard and Molnar, 1988), the gravitational instability of orogenic relief being driven both by stress field evolution at plate boundaries and by the thermal weakening and partial removal of the orogenic lithospheric root (Averbuch and Piromallo, 2012; Henk, 2000; Houseman et al., 1981; Morency et al., 2002; Platt and England, 1994; Rey et al., 2001). This late destabilization of the orogen implies a dynamic coupling between lithosphere-scale geodynamics (e.g., slab break-off, lithospheric delamination and related asthenospheric upwelling) and shallow tectonic processes (e.g., normal faulting and related flexural response) inducing a complex combination of areas undergoing rock uplift or subsidence (Dewey, 1988; Göğüş et al., 2016; Göğüş and Pysklywec, 2008; Ménard and Molnar, 1988; Platt and England, 1994). These coupled mechanisms have some direct implications on the reorganization of the drainage systems within the orogenic belt as well as spatial and temporal evolution of intramountain depositional and erosional patterns (Žák et al., 2018).

The thermo-mechanical configuration of the thickened orogenic lithosphere is a major parameter to take into account in this late orogenic tectonic collapse process (Le Pourhiet et al., 2004). The extensional reactivation of major thrust zones (also referred to as negative tectonic inversion) has been frequently shown as a basic mode of deformation in post-orogenic continental basins (Jolivet et al., 2010; Legrand et al., 1991; Malavieille et al., 1990; Minguely et al., 2010; Mohapatra and Johnson, 1998; Petersen et al., 1984; Powell and Williams, 1989; Smith and Bruhn, 1984; Stein and Blundell, 1990; Tari et al., 2023; Van Hoorn, 1987; Velasco et al., 2010; Williams et al., 1989). The relationships between extensional (or transtensional) faults controlling the tectonic subsidence and the underlying thrusts are, however, rarely fully constrained at depth. In this paper, seismic profiles from the late- to post-orogenic Lorraine Basin provide the opportunity to discuss the relationships between thrusts and normal faults during the collapse of the West European Variscan orogenic system.

Buried below the Mesozoic cover of the Paris Basin in NE France, the Lorraine Basin forms the western continuation of the Saar-Nahe Basin in SW Germany (figure 1). Such Lorraine-Saar-Nahe Basin (LSNB) developed within the Variscan orogenic system after the final mid-Carboniferous collision phase (Schäfer and Korsch, 1998; Schneider and Romer, 2010). This major intramountain basin represents the largest Permo-Carboniferous basin in Europe. It is bounded

to the north by the crustal-scale South-Hunsrück Fault (SHF) that closely follows the suture zone of the Rhenohercynian oceanic realm, between the northern Avalonian and southern Saxothuringian continental blocks (figure 1). This peculiar setting along the orogenic suture zone provides a major opportunity to record the late-stage dynamics of this European-scale subduction-collision system.

The Permo-Carboniferous successions of Lorraine and Saar regions (in France and Germany, respectively) were extensively investigated for coal exploration and mining during the last century (Courel et al., 1986; Donsimoni, 1981; Friedl and Siviard, 1932; Schäfer, 1989). More recently, crustal-scale seismic imaging was produced in the frame of the ECORS-DEKORP programs, at the northern and southern tips of the LSNB (figure 1); that is, the profiles DEKORP88 1C-9N and ECORS Vosges-Southern Rhine transect, respectively (Brun et al., 1992; Edel and Schulmann, 2009; Henk, 1993; Korsch and Schäfer, 1991; Weber, 1995). Despite such long-lasting geological and geophysical investigations, the tectonic development of the LSNB is still debated, and some inconsistencies remain regarding the kinematics of the main border fault zone and the different deformation phases (e.g. Korsch and Schäfer, 1995).

Geophysical exploration for oil and gas in the Lorraine Basin in the 1980s–1990s provided a large set of 2D seismic data to constrain basin geometries and kinematics at depth. Among this set of mostly unpublished seismic profiles, eleven selected profiles (representing 438 km) were reprocessed in the frame of the present study. The interpretation of the seismic profiles is calibrated by nine deep boreholes, allowing the construction of a 3D geological model with coherent stratigraphy, thereby leading to a revised structural framework and a new kinematical model for basin development. This paper focuses on the evidences of negative tectonic inversion of Variscan thrusts to explain the development of the Late Pennsylvanian (Stephanian)-Early Permian half-graben structures, the underlying Early to Middle Pennsylvanian (Westphalian) strata being involved in growth thrust-related anticlines during the syn-orogenic phase. The proposed model allows for the definition of a coherent structural evolution in the Lorraine and Saar-Nahe segments of the basin, accounting for the development of the main stratigraphic units and border fault system.

2. Geological Setting of the Lorraine-Saar-Nahe Basin (LSNB)

2.1 Variscan Tectonic Framework

The Permo-Carboniferous LSNB extends from SW Germany to NE France with a WSW-ENE lateral extent of about 300 km. It is about 100 km wide, and for a large part buried below the Triassic-Jurassic cover of the Paris Basin (Figures 1, 2). The LSNB forms a deep Late Paleozoic trough, filled

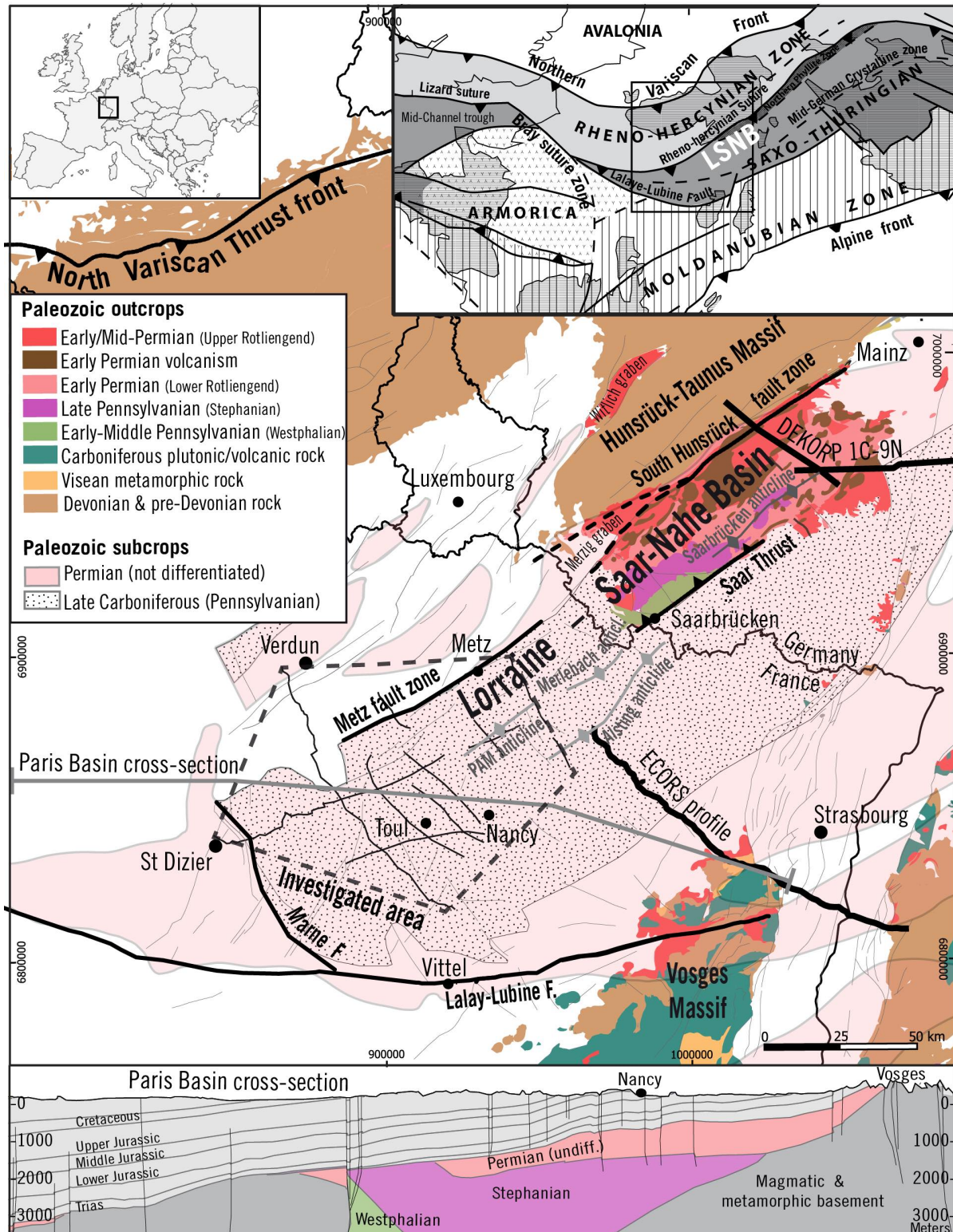


Figure 1. Geological map of eastern France and SW Germany, with the Mesozoic and Cenozoic sedimentary covers in transparency. The limits classically proposed for the Carboniferous-Permian subcrops at depth, are also reported (Delmas et al., 2002). Transects indicate the location of the ECORS and DEKORP seismic profiles as well as the Paris Basin cross-section represented below (Gély and Hanot, 2014). The inset map shows the location of the Lorraine-Saar-Nahe Basin (LSNB) within the main tectonic domains of the Variscan orogen (compiled from (Faure, 1995; Franke, 2014; Guillot et al., 2020; Schneider and Romer, 2010)).

by up to 8 km thick continental sediments deposited in fluvial to lacustrine environments (e.g. Schäfer, 1989; Schäfer and Korsch, 1998). Within the Variscan orogenic system, the LSNB represents a major intramountain basin located just south of the Rhenohercynian suture zone. The latter forms the surface trace of the southward subduction of the Rhenohercynian oceanic slab and of the adjoining distal southern continental margin of Avalonia (SW part of Laurussia) below the Saxothuringian-Moldanubian units of the upper lithospheric plate (the northern part of Gondwana; Averbuch and Piromallo, 2012; Edel et al., 2013; Franke, 2000; Oncken, 1997; Zeh and Gerdes, 2010). This suture is characterized by the northward thrusting units of the Northern Phyllite zone (SW Rhenish massif), a heterogeneous tectonic assemblage of rocks originating from the Devonian-Early Carboniferous Rhenohercynian-Avalonian passive margin oceanic shelf succession (Anderle et al., 1995; Franke, 2000; Oncken, 1997). These rocks were involved in the subduction zone but exhibit rather low peak-pressure conditions (i.e. only 6.5 kbar) indicating a limited amount of burial within the subduction channel before their exhumation (Massonne, 1995).

To the north of the LSNB, the Hunsrück-Taunus massif forms the internal part of the Variscan Rhenohercynian zone, dominated by folded and thrusting Early Devonian clastic shelf sediments, formerly deposited along the distal southern rifted margin of the Avalonian (Laurussia) continent (Oncken et al., 2000). To the south-east, the LSNB lies upon the units of the Saxothuringian retrowedge and more specifically on its northern border referred to as the Mid-German Crystalline Rise (MGCR). The latter represents a main site for syn-orogenic magmatism and the resultant relief, a significant clastic source for the LSNB toward the NW. Southward subduction and closure of the Rhenohercynian ocean indeed resulted in the formation of a late Devonian–mid Carboniferous magmatic arc on the northern flank margin of the Armorican-Saxothuringian microplate (Oncken, 1997). This magmatic arc formed a 75–100 km wide unit that can be traced along the strike of the suture zone over a distance of about 1,000 km. The Vosges and Black Forest Massifs are the exposed remnants of the MGCR in the area under study (Edel and Schulmann, 2009; Oncken, 1997).

2.2 Structural Development of the LSNB

The kinematic evolution of the LSNB is directly coupled with the geodynamics of the Rhenohercynian suture zone. In SW Germany, the South-Hunsrück border fault (SHF) bounding the Rhenohercynian thrust belt was first considered as a steep dextral strike-slip fault of 5–8 km of lateral offset associated with some significant transtensional component (Korsch and Schäfer, 1991; Schwab, 1987). Based on the interpretation of the DEKORP88 1C-9N seismic profile (Figure 1), this first-order major structure has been alternatively interpreted as a major listric normal fault that soles onto the suture zone at mid-crustal level, and resulting in the overall half-graben geometry

of the basin (Henk, 1993; Oncken, 1998). This crustal-scale normal fault is considered to have controlled the tectonic subsidence of the Saar-Nahe Basin from Early Pennsylvanian to Early Permian times (ca. 285 Ma). In addition, during the extensional phase, a series of NW-SE trending (about N130) transfer faults with inferred transtensional movements display a strong lateral segmentation of the basin, delimiting distinct depocenters with facies and thickness variations (Becker and Schäfer, 2021; Henk, 1992; Schneider and Romer, 2010; Stollhofen, 1998).

Such model of basin development, considering the long-term synrift tectonic subsidence of Permo-Carboniferous sequences was also proposed for the Lorraine segment of the basin, the Metz Fault being considered as the direct prolongation of the SHF (Courel et al., 1986; Donsimoni, 1981). The connection between these two faults was also considered in Korsch and Schäfer (1995) but the authors pointed out the inconsistency between the geometry of the Metz Fault delimiting the Lower-Middle Pennsylvanian coal-bearing strata in Lorraine and that of the SHF defined as a Late Pennsylvanian-Early Permian growth normal fault in the Saar-Nahe region. This inconsistency was attributed to an hypothetical along-strike migration driven by dextral strike-slip movement along the Metz-South Hunsrück fault zone (Korsch and Schäfer, 1995; Schäfer, 2011; Schäfer and Korsch, 1998). Although generally considered as a certainty, the direct connection between these two faults remains questionable. Originally, the Metz Fault was defined as a NW-dipping thrust rather than a SE-dipping normal fault (Guerrier and Pruvost, 1965). In addition, the western termination of the SHF is divided into two main branches, a northern one and a southern one delimiting the Merzig graben (Figure 1). The Metz Fault is assumed to correspond to the southern branch through a significant strike deviation, while the northern fault branch is not considered in the Lorraine segment of the basin. However, the gravimetric data and boreholes (e.g., Varennes and Vacherauville, (Figure 3)) suggest that the Upper Pennsylvanian-Lower Permian sequence largely extend north of the Metz Fault (Debrand-Passard, 1980; Delmas et al., 2002; Donsimoni, 1981).

Another point that is not fully accounted for by the model of continuous tectonic subsidence is the existence of a major unconformity between the Lower-Middle Pennsylvanian (Namurian-Westphalian) and Upper Pennsylvanian (Stephanian) to Lower Permian sedimentary successions, the lower one being considered to be affected by gentle folding and localized erosion (up to 1,000 m) before the deposition of the upper one (Korsch and Schäfer, 1995; Pruvost, 1934; Schäfer, 2011). The Lower-Middle Pennsylvanian strata exhibit a system of ENE-WSW trending folds relaying along strike (the Saarbrücken, Merlebach, Pont-a-Mousson (PAM) and the Alsting-Morhange folds), the forelimbs of which are locally affected by SE-verging thrusts. Based on localized subcrop data suggesting the involvement of Upper Pennsylvanian lay-

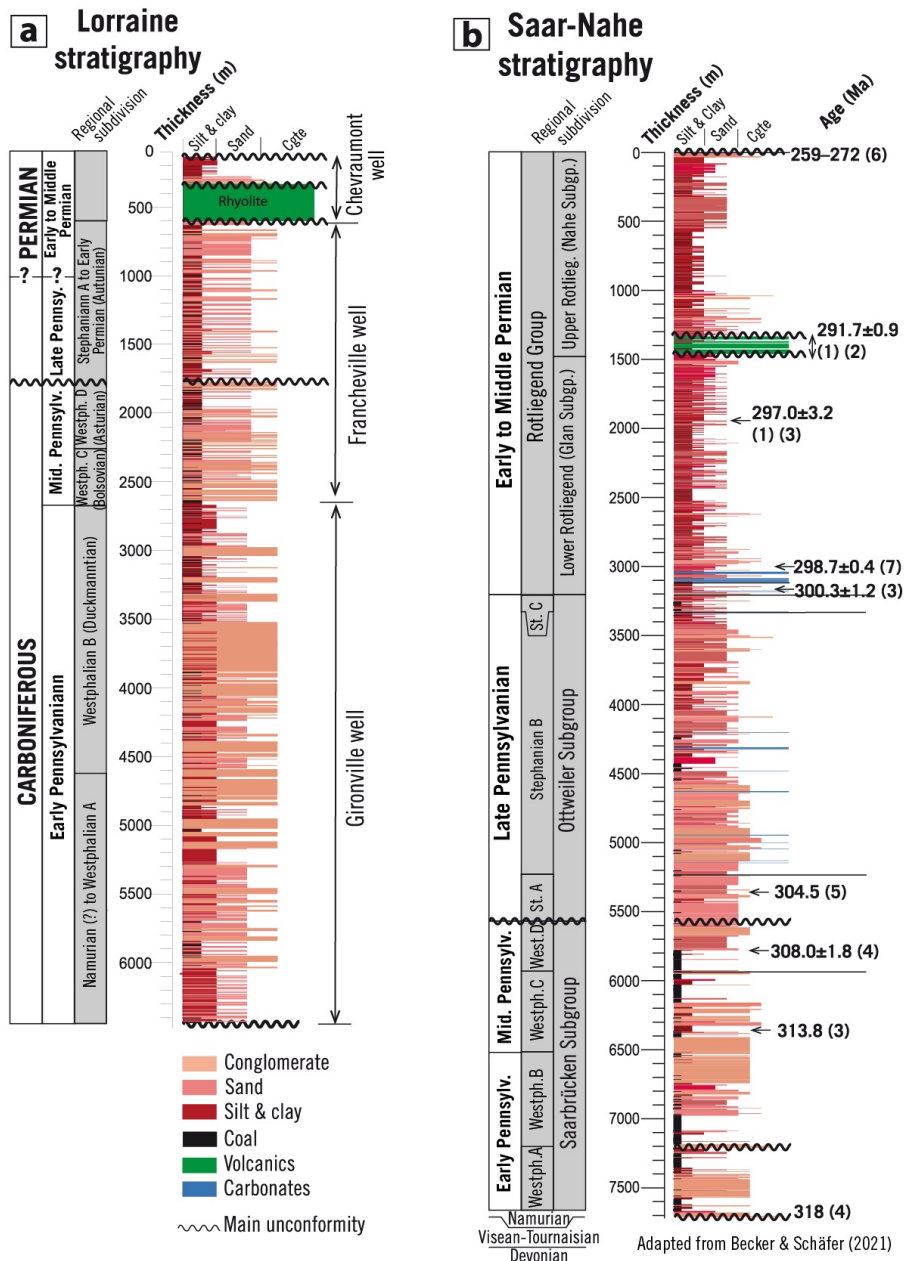


Figure 2. Synthetic stratigraphy of the Permo-Carboniferous Lorraine-Saar-Nahe Basin. The sedimentary log in the Lorraine segment of the basin is compiled from the Gironville, Francheville and Chevrumont wells. The sedimentary log in the Saar-Nahe segment is compiled from Saar, Olm, Monz, Landstuhl wells and field data (Becker and Schäfer, 2021). The stratigraphy is more developed in the Saar-Nahe segment of the basin with several time constraints – 4: Aretz et al. (2020); 3: Burger et al. (1997); 1: Königer and Lorenz (2002); 2: Königer et al. (2002); 5: Oplustil pers. com.; 6: Voigt et al. (2022)).

ers within fold-thrust structures (the Saar-1 borehole south of Saarbrücken in Germany; figure 1), the main folding and thrusting phase in the basin have been classically related to the Saalian shortening phase by late Early Permian times (Donsimoni, 1981; Kneuper, 1976; Pruvost, 1934, 1956). Vitrinite reflectance data within the coal beds (Early-Middle Pennsylvanian in age) involved in the Saarbrücken anticline (figure 1) clearly show however that for a given horizon, the reflectance is lower in the core of the anticline than in the adjacent syn-

cline thereby arguing for growth of the anticlines during the sedimentation (Hertle and Littke, 2000). The progressive migration of coal accumulation from the Merlebach anticline toward the syncline to the north of this structure provides another argument for such coeval development of sedimentation and folding in the Lorraine Basin (Donsimoni, 1981). To date, the kinematics of the compressional and extensional phases in the LSNB at the transition from the orogenic stage to the tectonic collapse stage is not fully understood.

2.3 Stratigraphy of the LSNB

The LSNB is a limnic intramountain coal basin without any connection with the sea, and differs from paralic coal basins located in Northern France, Belgium and Germany deposited in the foredeep of the northern Variscan thrust front (Schneider and Romer, 2010). The stratigraphy of the LSNB is well documented in outcrops in SW Germany, as well as in the Saar-1 borehole (Figures ??), which traverses the most complete Permo-Carboniferous succession (i.e., about 4.7 km thick) down to the Middle Devonian (Becker and Schäfer, 2021; Schäfer, 1989; Schäfer and Korsch, 1998). The rocks underlying the Carboniferous-Permian series consist of a slightly deformed and metamorphosed Mid-Devonian to Visean marine sedimentary sequence interpreted to have been deposited in a forearc position during the ongoing southward subduction of the Rhenohercynian slab (Oncken, 1997; von Seckendorff et al., 2004; Weber, 1995). The base of the basin is marked by a period of no deposition due to uplift of the MGCR units (320–335 Ma cooling age (McCann et al., 2006)) associated to the Variscan collision stage by mid-Visean times, locally referred to as the classic Sudetian phase (Kneuper, 1976; Weber, 1995). The initiation of the LSNB occurred during Early Pennsylvanian both in France and Germany, with increased subsidence from Middle Pennsylvanian (Korsch and Schäfer, 1995). The main sediment sources were located both in the Saxothuringian retrowedge to the South, and the Rhenohercynian prowedge to the North (Anderle, 1987; Oncken, 1997). It is however suggested that the main sediment sources change from N to S-SW, from Late Pennsylvanian times (Schäfer, 2011).

The Late Carboniferous stratigraphy is described here by using the Western European lithostratigraphic nomenclature and framework (Aretz et al., 2020; Lucas et al., 2022). Based on this nomenclature, the Early-Middle Pennsylvanian units is referred as late Namurian and Westphalian (Figure 2). The Westphalian succession (A, B, C, D) is based on the identification of paleobotanic markers (Alpern et al., 1969; Laveine, 1974; Pruvost, 1934). These substages correspond to the Langsettian, Duckmantian, Bolsovian and Asturian, respectively (Aretz et al., 2020). The limits of the Westphalian formations are however defined slightly differently in the Lorraine and Saar-Nahe segments of the basin (Figure 2). The Late Pennsylvanian Epoch (i.e., Stephanian in the classical Western European stratigraphic nomenclature) is divided into Cantabrian, Stephanian A, Stephanian B and Stephanian C. The stratigraphy of Lower Permian deposits is poorly constrained as it mainly involves undated continental red beds but it was classically divided into a lower Autunian and an upper Saxonian formation in the French part of the basin and lower Rotliegend and upper Rotliegend formation in the German part. Although poorly dated, these units are considered as roughly equivalent (Guerrier and Pruvost, 1965; Korsch and Schäfer, 1995). Such subdivision was set upon the geological time scale using dated interstratified volcanic layers in

Saar-Nahe (Königer et al., 2002; von Seckendorff et al., 2004). This Lower Permian sequence covers an about 299–270 Ma interval corresponding to Cisuralian and base Guadalupian time.

The sedimentary fill of the basin in the Saar-Nahe domain can be subdivided into four megasequences: (a) an initial Upper Namurian-Westphalian (Lower-Middle Pennsylvanian) series controlling subsidence mechanism of which still remains unclear and thereby commonly ascribed to a “proto-rift” phase; (b) a Stephanian (Upper Pennsylvanian) pre-volcanic synrift sequence; (c) a subsequent Lower Permian volcanic synrift sequence, (d) a final Lower Permian postrift sequence controlled by thermal subsidence (Henk, 1993; Korsch and Schäfer, 1991; Stollhofen, 1998). The classical “synrift” terminology is used in previous studies in the LSNB and also in this paper with regards to the mechanism of subsidence controlling the considered sequence that is, tectonic subsidence related to normal faulting.

The igneous rocks disrupting the thick continental succession include rhyolite, dacite and andesite distributed into superficial intrusions, lava flows and pyroclastic deposits that were mainly emplaced during Early Permian from 296 to 293 Ma (Königer and Lorenz, 2002; Königer et al., 2002; Lorenz and Haneke, 2004; von Seckendorff et al., 2004). During this event, normal faults controlling the subsidence of the Stephanian and Lower Permian synrift sequences were shown to be used locally as major conduits of magmas thus forming sorts of mega-dikes into the volcanic system (Lorenz and Haneke, 2004). Magma generation is attributed to underplating and intrusion of mantle-derived melts into the crust inducing its partial melting (Arz, 1996). This volcanic event is assigned to the base of the “Upper Rotliegend” sequence (Nahe Subgroup; Figure 2) and thereby would represent a magmatic pulse marking the transition toward the postrift thermal subsidence phase. In SW Germany (Figure 3), the Upper Pennsylvanian-Lower Permian layers are affected by the Saar Thrust, classically related to the Saalian phase by late Early Permian times (Donsimoni, 1981; Kneuper, 1976; Pruvost, 1934, 1956). This compression phase is suggested to cause up to 3,200 m of erosion in Saar-Nahe (Hertle and Littke, 2000), but a more limited amount of erosion (i.e., about 1,200 m) is estimated in Lorraine (Izart et al., 2016).

The stratigraphic scheme of the Lorraine segment of the basin was originally defined for the purpose of coal mining at the French-German border (Bertrand, 1930; Donsimoni, 1981; Friedl and Siviard, 1932; Pruvost, 1934). To the west of the coal mining area, deep boreholes document about 6 km of fluvial sediments deposited from Westphalian to Early Permian times (Figure 3). The Gironville well (5,683 m deep) documents the most complete succession (4.5 km) where the Westphalian series (up to 3.5 km thick) consists of conglomerates, sandstones, claystones with abundant coal beds. This series is characterized by fining-upward successions developed

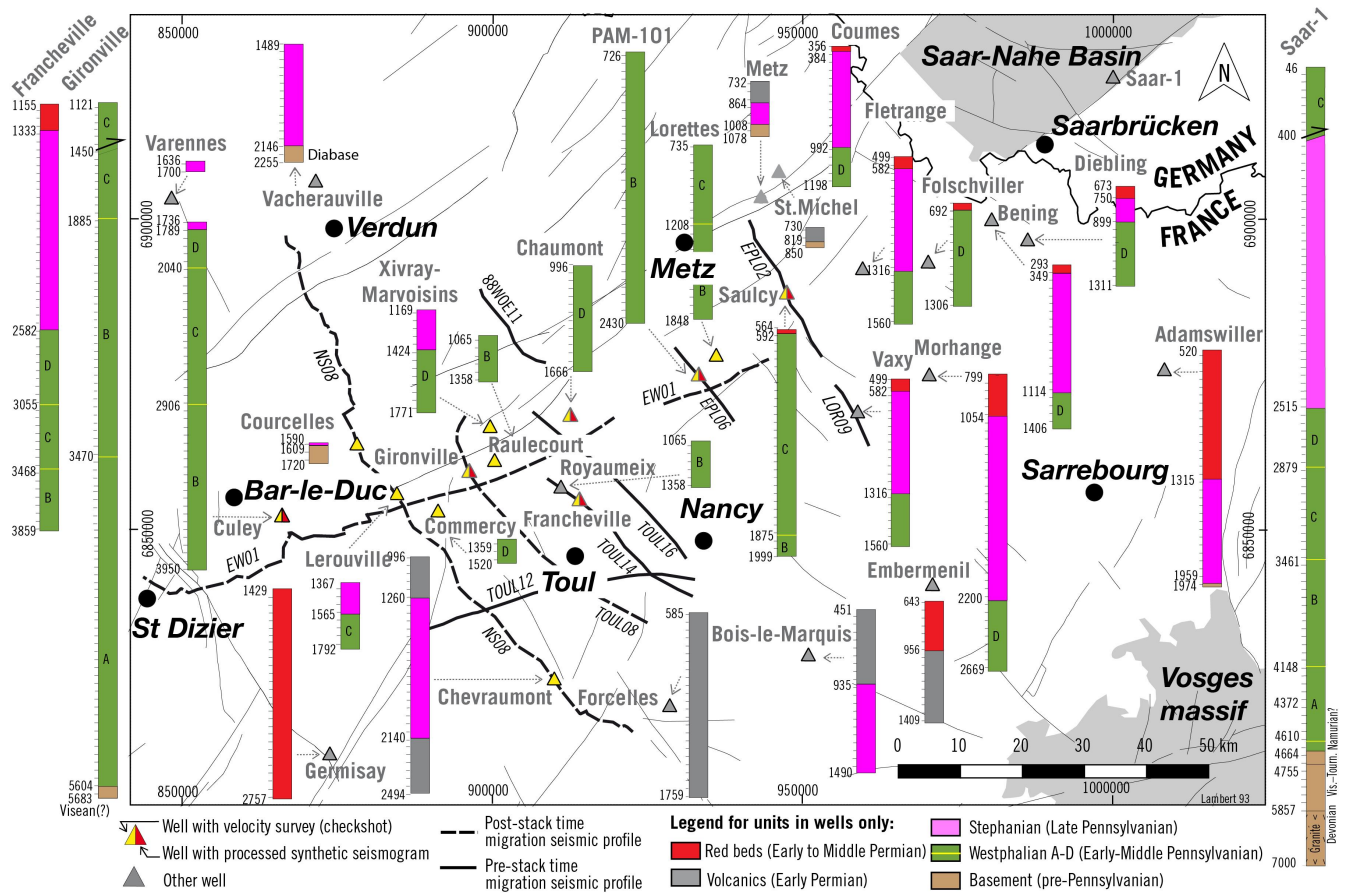


Figure 3. Location of studied seismic profiles and synthetic well data of the Permo-Carboniferous successions in the Lorraine Basin. Wells including velocity survey and synthetic seismogram are reported with colored triangles (see legend). Synthetic seismograms in Gironville and Francheville wells are presented in Figure 4.

in braided river environment (Fleck et al., 2001; Izart et al., 2005). These sequences are well defined in the Saulcy well and in the coal mining area, but they are not found further to the SW in Gironville, Culey and Francheville wells (Figure 3).

The Stephanian (Upper Pennsylvanian) deposits mainly consist of sandstone and claystone with minor occurrence of coal beds. This unit is best documented in the Coume and Francheville boreholes (Figure 3). The Westphalian and Stephanian strata are separated by an angular unconformity marking a sedimentary hiatus; the basin-wide deposition of the Holz conglomerates marks the resumption of sedimentation at the base of the Stephanian sequence (Bouroz et al., 1972; Engel, 1988; Weber, 1995). The stratigraphic gap at the base of the Stephanian unit (Cantabrian) corresponds to about 3 Ma between about 308.5 and 305.5 Ma (Burger et al., 1997; Knight and Álvarez-Vázquez, 2021; Schneider et al., 2020). The seismic data presented in the following sections, will show further evidence of the significance of this unconformity.

The Permian sequence is preserved with variable thickness (up to 1,400 m), intercalated with volcanic rocks in some

places. Rhyolites are found in the southern part of the basin (Figure 3). Andesite and trachybasalt are found in the northern Lorraine Basin, east of the Metz Fault. The Permian rocks are poorly dated in Lorraine and correlation with the Rotliegend Group is not clear. The “Lower Rotliegend” is not defined in Lorraine and the “Upper Rotliegend” red beds likely correspond to the “Saxonian” unit (Guerrier and Pruvost, 1965; Korsch and Schäfer, 1995). The Autunian (i.e., Lower Rotliegend) layers have not been documented in any well in the Lorraine area but their presence is likely at depth.

3. Seismic and Well Data

3.1 Seismic Acquisitions and Reprocessing

From the 1950s to the 1990s (but mostly in the 1980s), the Permo-Carboniferous Lorraine Basin was a target of significant onshore oil and gas exploration. These exploration surveys led to the acquisition of about 800 2D seismic reflection profiles representing a total length of about 9,000 km. Our study is based on the reprocessing of a selection of 11 2D seismic reflection profiles acquired in the 1980s and representing a total length of 438 km (Figure 3). They extend over the

whole Lorraine Basin, west of the former coal mining area “Houille res de Lorraine,” between Nancy, Toul and St Dizier cities (Figure 3). These seismic profiles oriented NNW-SSE and WSW-ENE intersects each other and crosscut the main fold structures and Upper Carboniferous to Permian series.

Given the CMP (Common MidPoint) gather acquisition parameters used in these exploration surveys, mainly the frequency bandwidth of the seismic source and the recording length (up to 4 s), we interpret reflectors up to 3.5 s TWT—corresponding to an estimated depth of 7 km below the reference datum surface with a vertical resolution of approximately 30–40 m. The 11 seismic profiles were reprocessed by the BRGM (“Bureau de Recherches Géologiques et Minier res”) between 2005 and 2017 to improve the quality of the images. Efforts were focused on three key steps, repeated several times throughout the processing sequence: (a) computation of primary and residual static corrections to remove the topographic and velocity effects of the shallow rock layer, (b) detailed velocity analysis, and (c) noise attenuation. Four profiles were reprocessed using the standard Post-Stack Time migration, and seven seismic profiles were reprocessed using the Pre-Stack Time migration method, enhancing the details of structural features and completing this reprocessing sequence before stacking (see [Beccaletto et al. \(2015\)](#) for further description of the procedure). The seismic profiles are generally of good quality despite the diversity of the seismic surveys, acquisition parameters and processing techniques. The presented seismic profiles are vertically exaggerated (with a factor of about 1.5) to facilitate the visualization of complete seismic profiles in the different figures.

3.2 Seismic-Well Tie

In addition to the seismic data, 13 deep exploration wells (source: Minergie database, <http://www.minergies.fr>) were used in order to provide geological information at depth. They were selected based on their proximity to the seismic profiles (less than 3 km), their total depth and drilled Paleozoic stratigraphy, and the availability of check-shot and well log data. The boreholes generally traverse the anticlines (Gironville, Chaumont, Chevraumont, Commercy, Courcelles, Culey, Lerouville, PAM, Royaumeix, Saulcy, Vaxy, Xivray-Marvoisins). The Francheville and Coume wells in the coal mining district, provided however, further documentation of the Stephanian (Upper Pennsylvanian) series (Figure 3).

We calibrate and tie the key seismic markers to their corresponding geological surfaces. Nine out of the 13 wells contain velocity data that were used to convert the wells from depth (in m) to time (TWT), and then to correlate the geological markers with the seismic reflectors. Six out of the thirteen wells (Chaumont, Culey, Francheville, Gironville, PAM and Saulcy; see location in Figure 3) can be used to calculate synthetic seismograms (Figure 4). A synthetic seismogram

is a theoretical seismic trace that illustrates the variations of acoustic impedance in the different rock layers along a given borehole. It is generated by convolving the reflective coefficient computed from sonic and density logs, with a seismic wavelet best representing the seismic signal close to the well. These boreholes are located in the vicinity of the seismic profiles and meet the following requirements: availability of velocity data to calculate a synthetic seismogram (sonic log and velocity survey), and sufficient interval within the Paleozoic series.

Synthetic seismograms were generated following several steps: (a) quality control of the sonic log and removal of aberrant values; (b) correction of the drift of the sonic log and integration of sonic log with check-shots; (c) generation of a time-depth chart converting the vertical scale of the well data from depth to time using integrated velocity data; (d) computing the density value according to Gardner’s law ([Gardner et al., 1974](#)); (e) computation of the acoustic impedance; (f) computation of the reflectivity coefficient; (g) generation of a seismic wavelet extracted from the seismic traces around the well; (h) convolution of the reflectivity coefficient with a seismic wavelet. Once the synthetic seismograms were created, and they were correlated with the adjacent segments of seismic profiles so that they fit the seismic signal around the well, completing the seismic-well tie process (Figure 4).

Synthetic seismogram and seismic-well tie enable to identify the key geological surfaces and geometry of the main seismic units (Figure 4). The interpretation of the 2D seismic profiles was carried out using SKUA-GOCAD software. From top to bottom, the main geological boundaries are defined as: the Top Paleozoic Unconformity (TPU) or base of the Triassic sequence; the base of the postrift sequence (late Early Permian); the base of the synrift sequence or Base Stephanian Unconformity (BSU). The apparent base of the Lorraine Basin is defined as the Base Westphalian Surface (BWS). This sequence appears decoupled from its substratum in the SE part of the basin; thereby the BWS corresponds here to a decollement at the base of the basin.

4. Seismic Interpretations

4.1 Overview of the Main Seismic Features and Facies

The first-order seismic features and units observed on these seismic profiles are presented in Figures ?? and are described below. The Mesozoic cover of the Paris Basin consists of parallel to sub-parallel continuous reflectors with medium- to high-frequencies and alternating medium- to high-amplitudes related to lithological variations within the Triassic and Jurassic units. These reflectors dip gently westward with exposed strata that are older to the east (Permian and Triassic series) than in the investigated area (Jurassic series).

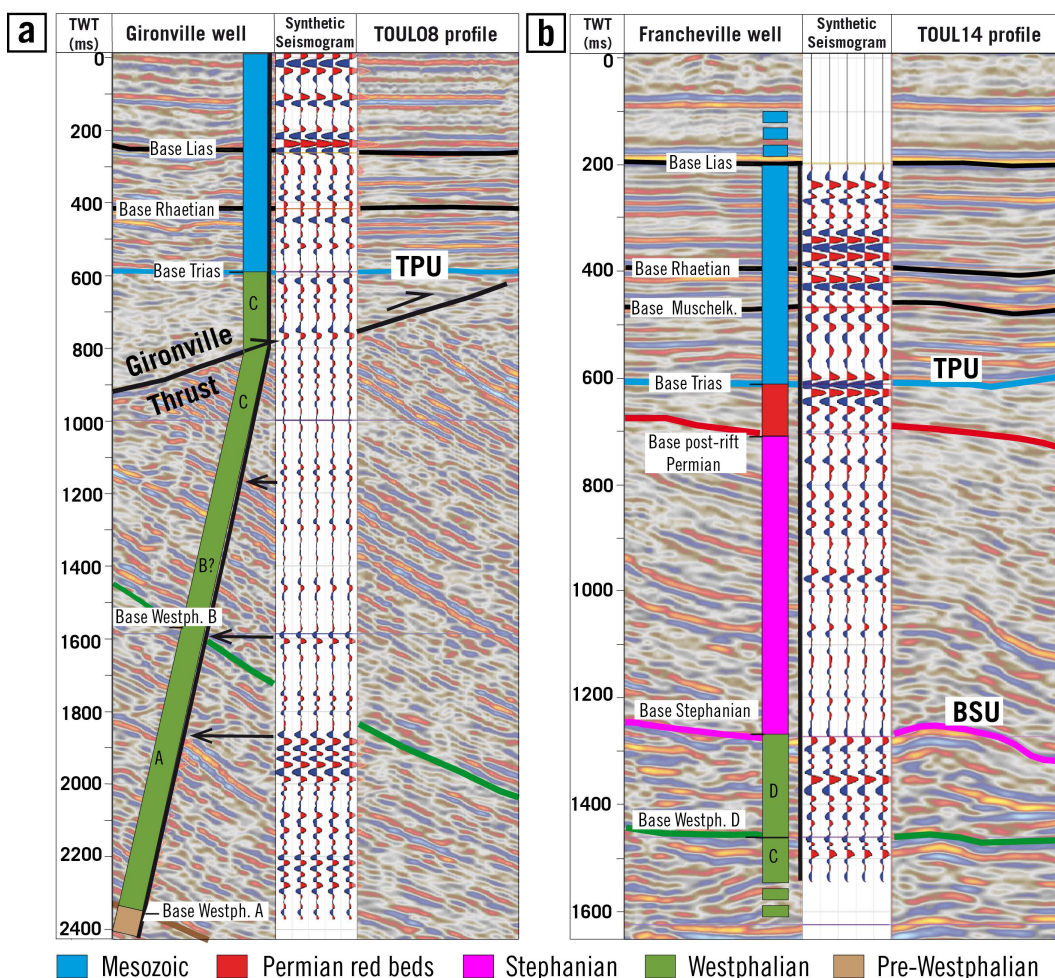


Figure 4. Seismic-well tie (a) between the Gironville well and the TOUL08 seismic profiles, and (b) between the Francheville well and the TOUL14 seismic profile. The Gironville well is the only well reaching the base of the Westphalian succession in Lorraine. The Francheville well traverses the Base Stephanian Unconformity (BSU).

One of the most visible features on all the seismic profiles is the TPU lying around 0.5–1.0 TWT (about 750–1,500 m deep) in the investigated area. The TPU clearly truncates the Paleozoic reflectors below the parallel and continuous Triassic reflectors. The underlying Lower to Middle Permian unit, defined as postrift in the Saar-Nahe segment of the basin (Henk, 1993; Korsch and Schäfer, 1991; Stollhofen, 1998), represents a relatively thin succession (few 100's ms TWT). It is represented by low-energy and rather transparent facies, with weakly continuous reflectors. More locally, the chaotic and highly reflective seismic facies correspond to volcanic rocks (mostly rhyolite and andesite) at the base of the Permian postrift unit.

The underlying Stephanian to Lower Permian unit, defined in the Saar-Nahe segment of the basin as synrift is related to low- to high-amplitudes reflectors that appear mostly continuous and parallel, probably in relation with internal lithological variations. It forms localized zones of increased thickness beneath the postrift Permian unit or directly the TPU. The

thickness of this unit increases significantly toward the west of the study area where it reaches 2.2 s in thickness (about 4,500 m).

The other striking seismic feature visible on our newly reprocessed seismic data set is the angular unconformity (BSU) between the folded Westphalian and Stephanian units. The thick Westphalian unit (about 4 km thick) can be observed either directly beneath the Mesozoic cover, the postrift unit or the synrift unit. It corresponds to the high-amplitude, low frequency, semi-continuous to continuous, planar to undulating reflectors. The amplitude of the reflectors varies laterally and seismic facies do not allow to clearly identify subunits.

In a general way and independently of the quality of the raw data, some chaotic seismic facies are explained by the presence of volcanic rocks. The latter are preferentially localized in the footwall of normal faults limiting to the SE the synforms preserving Stephanian-Lower Permian sequences as well as in the vicinity of the Metz fault zone (Figures

6 and 7). As shown in exposed volcanic systems from the Saar-Nahe segment of the basin (Lorenz and Haneke, 2004), such configuration strongly supports the fact these faults were used as conduits for magma migration toward the surface during the late synrift volcanic phase (ca. 296–293 Ma BP von Seckendorff et al., 2004). The precise geometry of the Permo-Carboniferous units as well as the main structures controlling the different depocenters and their deformation are further described in the following sections. Presented structural interpretations basically rely on the geometry of reflectors but as promoted by recent studies on the evaluation of conceptual uncertainties when interpreting seismic data (Bond et al., 2012) the kinematical consistency of structures both at the section-scale (2D) and between different adjacent profiles (3D) must be considered. This approach was particularly useful in zones where the seismic profiles are of poor quality below the TPU (e.g., NW part of NS8 and 88W0E11 profiles and SE part of the TOUL08 profile; Figures 6 and 7).

4.2 Evidence for the Syn-Orogenic Character of the Westphalian Unit

The Westphalian unit is characterized by several adjacent anticlines and synclines, imaged in most of the NW-SE seismic profiles. In the eastern part of the basin, these anticlines form prominent structural highs (PAM and Alst- ing anticlines, Figure 5), truncated by the TPU. The longitudinal WSW-ENE seismic profile EW01 (Figure 8) follows the main axis of the Westphalian anticlines and shows poorly preserved Stephanian and Permian layers.

A major point, emphasized by this new set of seismic profiles is that the Westphalian anticlines are clearly truncated by the BSU (Figures 5,6,7), thus demonstrating their subaerial exposure and denudation as the folds developed (or at least as they formed structural relief before the onset of the subsidence controlling the deposition of the Stephanian deposits). Well data, dominantly located in the core of the Westphalian anticlines (Figure 3) are correlated with the intersecting seismic profiles to identify the Westphalian subunits (noted A, B, C and D). A very striking point is the peculiar geometry of internal reflectors of Westphalian C and D in the forelimb of the anticline, as highlighted on the profile EPLY02 (Figure 5): the latter shows some significant convergence of reflectors in Westphalian C and D layers toward the anticline hinge suggesting that they developed as growth strata within the forelimb of the fold. The forelimbs of anticlines are also disrupted by NW-dipping thrusts, identified for the first time in the Lorraine Basin, and exemplified in the Gironville area (profiles TOUL08 and TOUL16, Figures 6b and 7). We identified three other main thrusts, namely the Metz, PAM and Morhange thrusts. The Metz and Gironville thrusts are located in the northern part of the area and form the north-western limit of the Westphalian depocenters (profiles NS08 and W0E11-TOUL16; Figure 7). Both PAM and Morhange

thrusts form intra-basin thrusts (profiles EPLY02-LOR09; Figure 5). The relationships of these intra-basin thrusts with the syn-sedimentary growing folds suggest that the latter developed as fault-propagation folds accommodating progressive shortening transferred to shallow crustal levels.

As previously described along the ECORS Vosges-Southern Rhine transect (Edel and Schulmann, 2009), the SE termination of the Westphalian layers form an overall stratal pinch-out, marked by onlaps of strata onto high amplitude N-dipping reflectors (Figures 6 and 7a). This planar and gently dipping surface (about 15° toward the NW), is ascribed to BWS at the base of the basin. It is well defined above 3.0 s TWT in most of the seismic profiles. Within this SE part of the basin, all faults traces root down onto this surface. Such geometry clearly indicates that BWS forms a decollement level, active during thrust propagation into the basin and reactivated during subsequent deformation.

4.3 Negative Tectonic Inversion and Its Control on the Development of synrift Depocenters

In the central part of the basin (Toul-PAM-Nancy area; Figures 1 and 3), the folded reflectors (Westphalian unit) abruptly terminate upward against the base of the Stephanian strata, forming an angular unconformity, which is clearly observed in profiles TOUL14, TOUL08, TOUL16 and EPLY02 (Figures 5–7). Several continuous and high amplitude reflectors are traced within the Stephanian succession. Although poorly dated and not correlated to a particular stratigraphic limit, these continuous reflectors are used as surface markers to ent individual depocenters are parallel and dominantly tilted toward the SE (TOUL14, TOUL08, TOUL16, EPLY02; Figures 5,6, 7b). To the south, these overall SE-dipping reflectors form localized synclinal hinges against some discontinuities strongly dipping to the NW, interpreted as normal faults delimiting to the SE the Stephanian-Lower Permian depocenters. In the TOUL08 and TOUL14 profiles, they correspond to sharp limits with a poorly reflective and chaotic seismic unit (Figure 6). The significant downthrow of this unit by normal faulting is associated with the occurrence of drag folds into the Stephanian to Lower Permian layers (see e.g., TOUL08 in 6b). Such extensional folds have been classically observed in rift-related basins and frequently interpreted as the result of fault propagation into the synrift sequence (e.g. Gawthorpe et al., 1997; Janecke et al., 1998; Sharp et al., 2000; Tavani et al., 2013; Withjack and Olson, 1990). Taking into account the structural context of the Stephanian-Lower Permian sequence in the nearby Saar-Nahe domain, the syn-depositional development of these drag folds is likely but a post-depositional origin cannot be however totally excluded.

Several normal faults are identified: the Lesmenils, Toul, Chevaumont and Meligny normal faults (Figures 5-7. Most of them appear to connect onto the BWS at depth (TOUL14, TOUL08, TOUL16, NS08; Figures 6 and 7). In the central

**A Deformed Wedge-Top Basin Inverted During the Collapse of the Variscan Belt:
The Permo-Carboniferous Lorraine Basin (NE France) — 12/28**

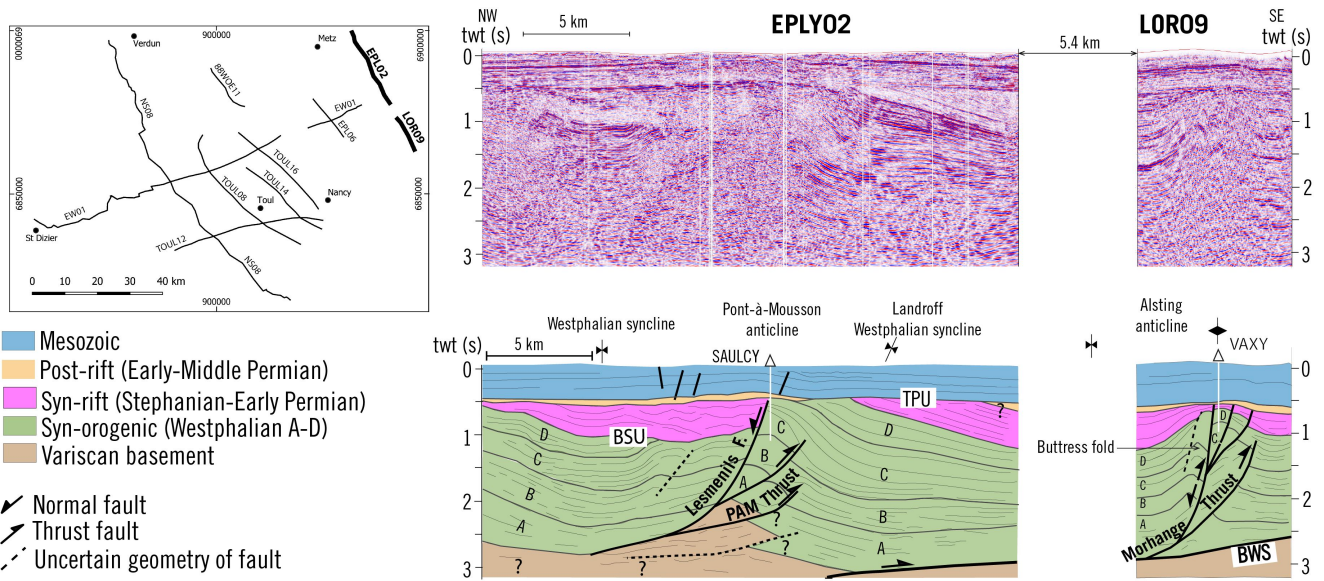


Figure 5. Reprocessed NW-SE trending seismic profiles EPLY02 and LOR09 (both uninterpreted and interpreted) illustrating the fold-thrust interactions and the syn-orogenic character of the Lower-Middle Pennsylvanian (Westphalian) layers within the eastern part of the Lorraine Basin. TPU, Top Paleozoic Unconformity; BSU, Base Stephanian Unconformity; BWS, Base Westphalian Surface. Note the growth-structure type geometry on the Westphalian layers in the forelimb of the Pont-a-Mousson (PAM) anticline.

part of the basin, the NW-dipping Lesmenils normal fault is located in the hangingwall of the PAM Thrust and limits to the SE a poorly preserved Stephanian depocenter resting unconformably onto underlying folded Westphalian layers (profile EPLY02, Figure 5). The NW-dipping Toul normal fault and its westward prolongation after localized lateral transfer, the Chevaumont normal fault, limit the main Stephanian to Lower Permian depocenter of the investigated area referred to the Francheville depocenter (Figures 6 and 7). The latter and the one located north of the Lesmenils Fault, thereby appear as the remnants, after severe denudation, of some asymmetric half-graben structures controlled by NW-dipping normal faults, that is, antithetic to the main border fault at the NW limit of the basin. The footwall blocks of the Toul and Chevaumont normal faults are poorly imaged due to poor seismic reflectivity and chaotic geometry of the reflectors. As we mentioned previously, this situation is likely due to the presence of late synrift volcanic bodies intercalated in the sedimentary successions (Early Permian in age, ca. 296–293 Ma BP) that used the normal faults as conducts for their migration toward the surface (Lorenz and Haneke, 2004). The Chevaumont well is located in the hangingwall of the Chevaumont Fault, and traverses two rhyolitic bodies that are 258 and 361 m thick respectively (Figure 3). In this western part of the investigated area, the northern border of the Francheville depocenter, is affected by a second-order SE-dipping normal fault with restricted displacement, the Meligny normal fault (Figure 7).

An important observation is that half-grabens localizing remnants of Stephanian-Lower Permian sequences are specif-

ically located along the crest and backlimb of former thrust-related anticlines. Considering an individual extensional depocenter, the zone of maximum thickness lies above the zone of maximum denudation of the underlying anticlines (up to the base of Westphalian B in TOUL14 profile; Figure 6). Such observation implies that the zone of maximum subsidence during normal faulting is superimposed to the zone that initially localized maximum rock uplift during the development of the thrust-related anticlines thereby featuring a characteristic negative tectonic inversion process. The normal faults clearly root down onto ramps of thrusts or directly onto the BWS. In map view, normal faults controlling depocenters are noticeably aligned parallel to the underlying thrusts (Figure 8). Such overall geometry shows that thrusts were reactivated along the deepest parts of their surface (Figure 5). Such configuration is characteristic of negative inversion of thrust structures, normal faults classically short-cutting the upper flat of thrusts and connecting at depth the footwall ramp or the basal decollement, thereby conferring a listric geometry to the normal faults (Averbuch et al., 1992; Minguely et al., 2010; Mohapatra and Johnson, 1998; Smith and Bruhn, 1984; Tavarnelli, 1999; Williams et al., 1989) With regard to the dynamics of the tectonic inversion process, a very striking point of the observed geometries is the lack of clear evidences of significant fan geometries toward the normal faults as it is typically observed in synrift series. Only the NS08 profile (Figure 7), which displays the thickest remnant of the Stephanian-Lower Permian sequence (ca. 4,500 m), suggests such a (subtle) fan structure. In this area, the thickness of the Stephanian sequence within the Francheville depocenter significantly decreases toward the NW, that is, outward the main Chevaumont normal fault

**A Deformed Wedge-Top Basin Inverted During the Collapse of the Variscan Belt:
The Permo-Carboniferous Lorraine Basin (NE France) — 13/28**

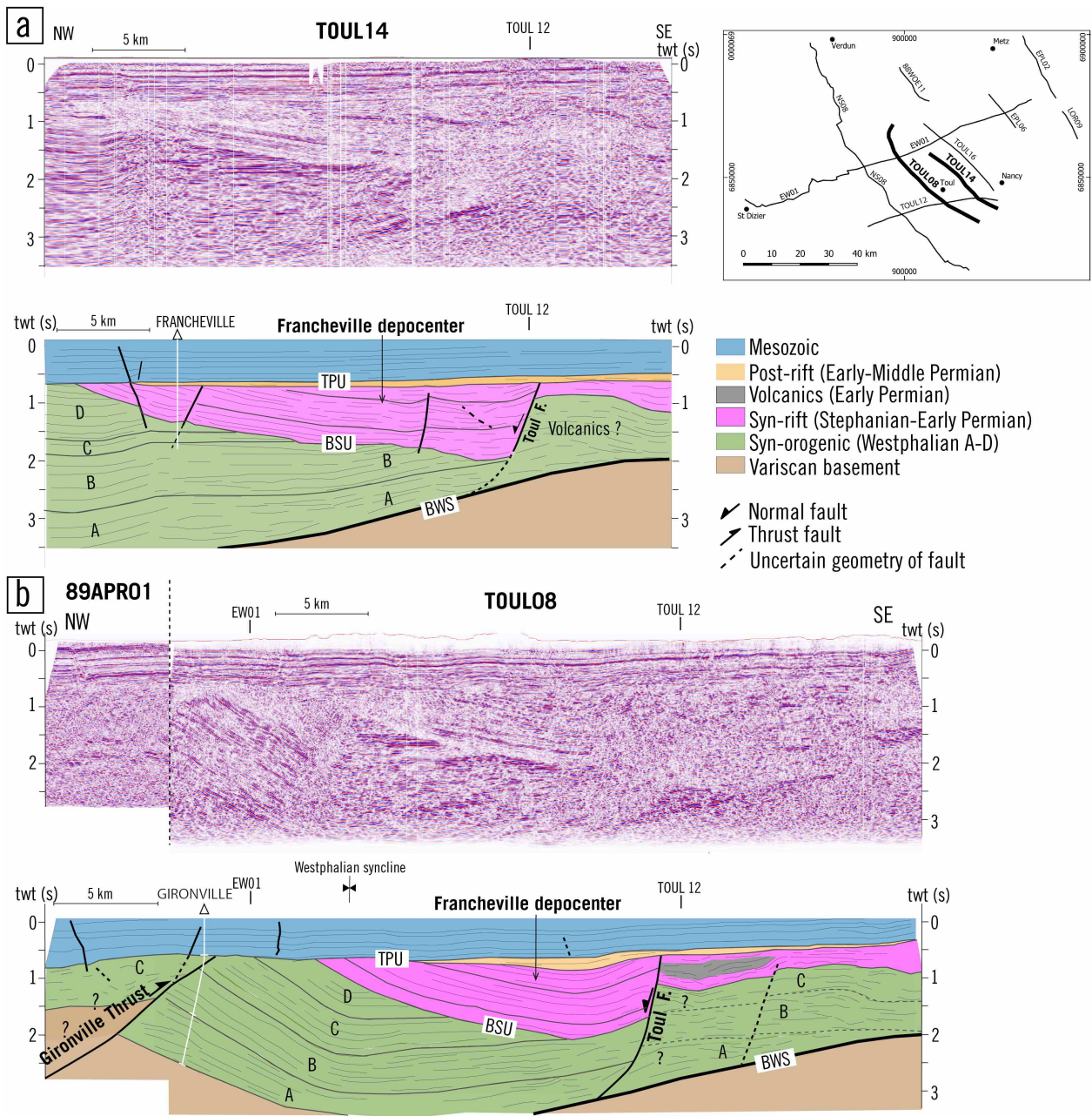


Figure 6. Reprocessed transverse seismic profiles (a) TOUL14 and (b) 89APR01-TOUL08; uninterpreted and interpreted. These profiles clearly emphasize the Base Stephanian Unconformity (BSU). Note also the maximum thickness of the synrift depocenter (Stephanian-Early Permian) onto the most deeply eroded part of the folded Westphalian succession thereby featuring a major topographic and tectonic inversion process.

that forms the lateral equivalent of the Toul normal fault after displacement by the lateral Commercy transfer fault. This point clearly appears on the profile NS08 (Figure 7) although some second-order SE-dipping faults (such as the Meligny fault) make the NW border of the depocenter slightly more complex than that observed laterally on the TOUL profiles (Figure 6). Taking this point into account, we emphasize the possible impact of the denudation of the NW part of these depocenters in the apparent lack of thickness change.

More generally, the limited lateral thickness variations of the synrift layers have to be considered with regard to the structural position of these depocenters into the basin. They are actually controlled by NW-dipping normal faults that represent antithetic faults to the main border fault at the northwestern side of the basin; that is, the SHF and its prolongation in the Lorraine segment of the basin. In the investigated area, the SE-ward thinning of synrift strata due to the overall

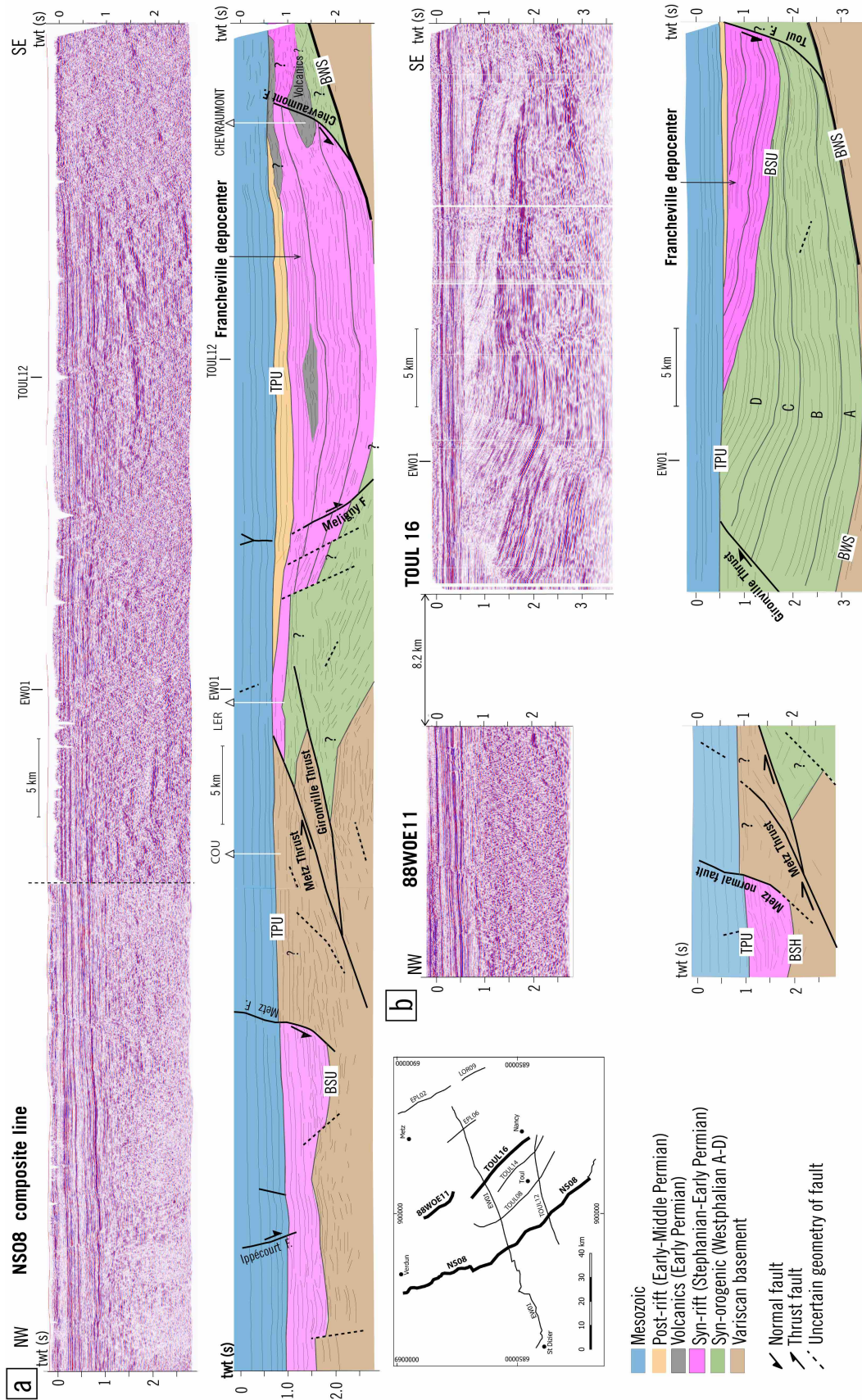


Figure 7. Reprocessed NW-SE trending seismic profiles (a) NS08 and (b) WOE11-TOUL16; uninterpreted and interpreted. These profiles particularly emphasize the geometry of the northern limit of the Westphalian basin delimited by the Metz Thrust. Note also the significant increase in thickness of the synrift depocenter in the NS08 profile, in the western tip of the Lorraine Basin.

half-graben structure (as shown by the growth syncline geometry observed in the DEKORPIC-9N profile; (see [Henk, 1993](#); [Oncken, 1998](#)) is presumably compensated by NW-ward thinning associated to the coeval displacement on the observed antithetic (NW-dipping) normal faults. Such geometry is perfectly well characterized by analog modeling experiments of synrift sedimentation associated to half-graben development upon major listric normal faults ([McClay, 1990](#); [Tari et al., 2023](#); [Ouzgait et al., 2010](#)).

Although not recorded by significant thickness changes in the Stephanian-Lower Permian series, our seismic profiles clearly point out the typical geometry provided by the extensional reactivation of thrusts, inducing the collapse of the backlimb of previously developed thrust-related anticlines and controlling the development of Stephanian-Lower Permian depocenters only at the back of the pre-existing anticlines. Noteworthy, such typical geometry, clearly expressed in the investigated area, perfectly fits the values of vitrinite reflectance into Westphalian layers from the Saarbrücken anticline. Within a same Westphalian horizon, the reflectance have clearly been shown to be lower in the core of the anticline than in the synform at the back of the anticlinal (Pryms synform) thus arguing for enhanced burial and sedimentation in the synform area ([Hertle and Littke, 2000](#)). Collapse of the backlimb and associated synrift deposition during Stephanian-Early Permian is a valuable mechanism to account for such vitrinite reflectance distribution.

4.4 Transverse Faults

The thickness of the synrift unit (Stephanian-Early Permian) increases toward the west to reach up to 2.2 s TWT (about 4,500 m in thickness) in the western part of the TOUL12 profile (Figure 8). The BSU surface is progressively downthrown by transverse faults striking N130-150, sub-parallel to the Marne Fault (Figure 7a; Figure 8a). These transverse faults named as Delme, Nancy and Commercy faults display a strong dip either to the NE or SW with apparent normal displacement on seismic profiles. These faults have been already mapped by previous investigations but their significance in the context of the tectonic inversion and post-orogenic extension was not understood ([Donsimoni, 1981](#)). The seismic profile EW01 (Figure 8b) displays such transverse faults delimiting horst and graben structures along the axis of the Westphalian anticlines (Figure 8). The trace of the Nancy Fault is not imaged in seismic profiles, but the fault is deduced by significant offset of the Westphalian unit (0.5–0.6 s TWT, representing about 1,000 m of apparent displacement). The Commercy Fault is the best-defined transverse fault within our data set, observed in the western part of the basin in both EW01 and TOUL12 profiles (Figure 8). This fault roots onto the BWS decollement level in the southern part of the basin (TOUL12, Figure 8a) but appears to displace it in profile EW01 (Figure 8b). Such situation can be explained by the fact that the decollement deepens toward the NW and ramps down into the

basement in the Metz area.

4.5 Local Reactivation During the Early Permian Saalian Compressive Phase

Apart from the westernmost depocenter (west of Commercy Fault), the synrift unit (Stephanian-Early Permian) appears notably truncated below postrift unit or directly the TPU. Such significant erosion, evidenced at the basin scale can be ascribed to rock uplift during the Saalian compressive phase ([Donsimoni, 1981](#); [Hertle and Littke, 2000](#); [Izart et al., 2016](#); [Kneuper, 1976](#); [Pruvost, 1934, 1956](#)). There is however little evidence in the seismic profiles for the involvement of the Stephanian layers in thrust structures as considered in classical interpretations. Such involvement can be only suspected within the forelimb of the Alsting anticline in the southeastern part of the Lorraine Basin, in the footwall of the Morhange thrust zone (see LOR09 seismic profile, Figure 5). In this zone, the BSU is not strongly expressed and the Stephanian layers seemingly onlap the pre-existing Alsting anticlinal ridge developed during the Westphalian compression before being tilted and locally thrustured (Saalian reactivation of the Morhange thrust). The existence of a buttress fold against a normal fault in the backlimb of the Alsting anticline (Figure 5) suggests that the compressional reactivation occurred after the development of the synrift sequence, probably during the Saalian phase by late Early Permian times (ca. 285 Ma).

The low amplitude of displacement and deformation with regard to the Westphalian strata suggests a limited reactivation of the Morhange Thrust during the Saalian phase. The reactivation of late Westphalian thrusts and local positive tectonic inversion of normal faults are suggested to result in the general doming of the basin and partial erosion of pre-Saalian structures, but it only represents a second-order deformation event.

4.6 Geometry of the Basin Bounding Faults

The northern border of the Carboniferous to Permian Lorraine Basin is commonly defined by the Metz fault zone that separates at depth Variscan basement rocks from the coal-bearing successions ([Donsimoni, 1981](#); [Kneuper, 1976](#); [Pruvost, 1934, 1956](#)). This interpretation results from the direct extrapolation of observations made along the SHF in Saar but is based on a restricted set of deep boreholes. The profiles NS08 and WOE11-TOUL16 (Figure 7) provides the first opportunity to image the Metz fault zone. Despite the poor quality of the seismic image below the TPU, reflectors do not display the geometry expected to represent a major SE-dipping normal bounding fault as defined in Saar-Nahe ([Henk, 1993](#); [Oncken, 1998](#)). Conversely, normal faults, well defined on the seismic profiles in the Mesozoic cover clearly dip to the NW. This is also the case for a set of high-amplitude reflectors in the underlying Paleozoic units. Seismic reflectors in the SE-dipping strata abruptly stop against this set of NW-dipping reflectors. The latter are thereby interpreted as the trace of a major SE-verging thrust fault zone rather than a SE-dipping

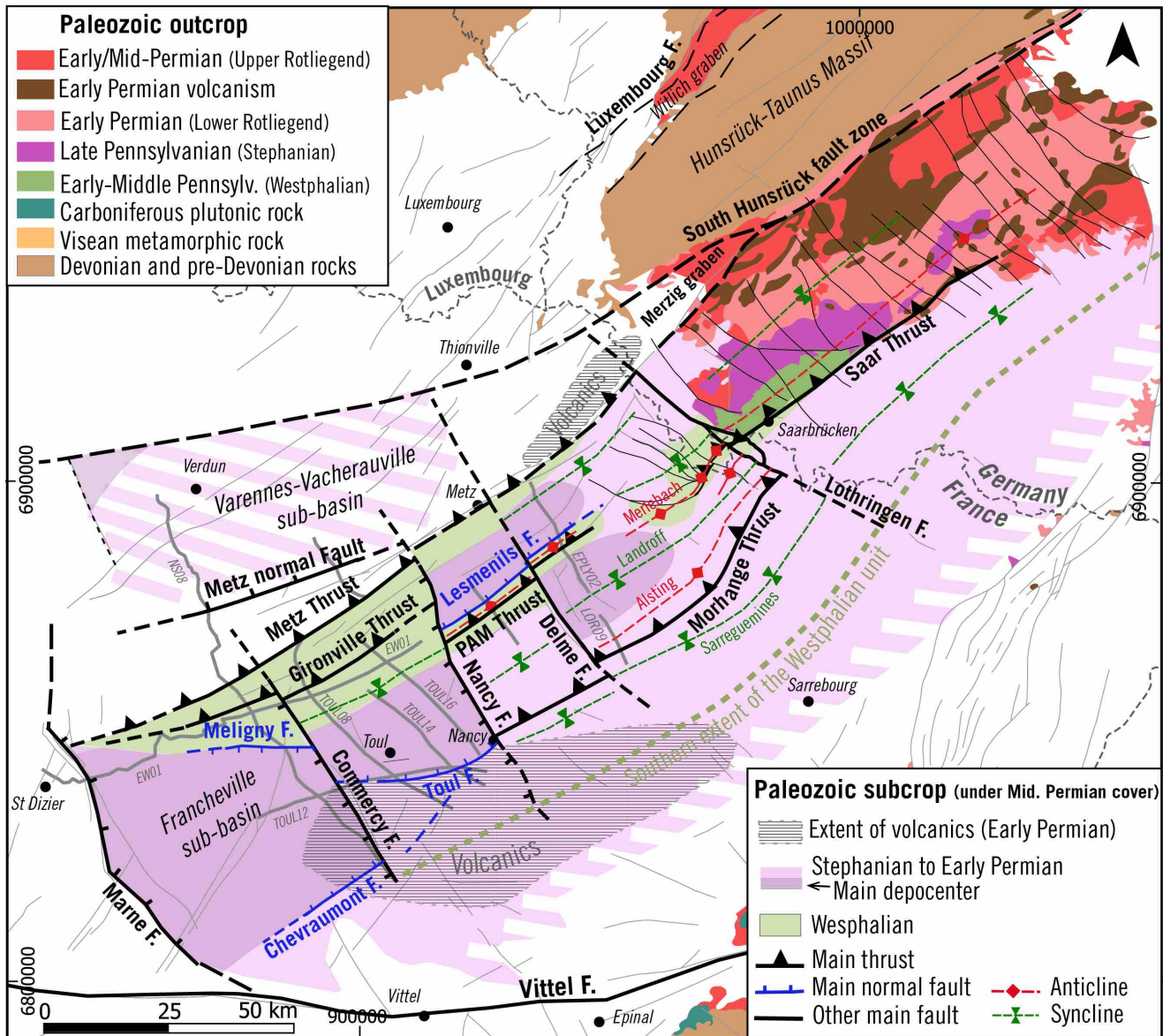


Figure 9. Revised structural map of the Permo-Carboniferous of the Lorraine-Saar-Nahe Basin (LSNB) (geological map based on [Chantraine et al. \(2003\)](#); [Schäfer \(2011\)](#)). The structural map in the central part of the LSNB is based on [Donsimoni \(1981\)](#). Our seismic interpretations enable to propose a new structural map in the westernmost part of the LSNB, as well as new definition of its structural limits.

normal fault. It is defined here as the Metz Thrust, emplacing Variscan basement rocks upon the folded Westphalian series (Figure 7). As emphasized in the TOUL08 and TOUL16 profiles, a second-order thrust defined as the Gironville Thrust, also affects the Westphalian series in the footwall of the Metz Thrust (Figures 6 and 7). Both thrusts probably link at depth.

It is of importance to note that the Metz Thrust does not correspond to the Metz normal fault traced within the Mesozoic cover and located further to the NW (10–20 km) in the hangingwall of the Metz Thrust (NS08, WOE11; Figure 7). The Metz normal fault display a strong NW dip and delimit

its at depth an extensional depocenter (Stephanian to Early Permian) that can reach up to 1.0 s TWT in thickness (about 2,000 m). It also affects, to a lesser degree, the overlying Mesozoic strata. Thus this normal fault accommodated Late Paleozoic extension and was later slightly reactivated in the Mesozoic (Le Roux, 2000). The Metz normal fault may connect at depth to the Metz Thrust at about 3.0 s TWT (Figure 7). The western end of the Lorraine Basin is not clearly imaged in our seismic data set. However, as defined in previous studies ([Delmas et al., 2002](#); [Le Roux, 2000](#)), the E-dipping Marne Fault is likely (see the western border of the composite profile EW01 in Figure 8). As observed for the Metz normal fault, it

also affects to a lesser extent the Mesozoic cover thus arguing for its reactivation during the development of the Paris Basin. The SE termination of the basin is also poorly imaged in most of our profiles due to the presence of volcanic bodies. As previously documented on the ECORS-DEKORP profiles (see [Edel and Schulmann, 2009](#)) and corroborated by the LOR09 and TOUL08 profiles (Figures 5 and 6), the basin thins toward the SE forming an overall sedimentary pinch-out above the BWS. Westphalian reflectors unconformably overlie the BWS, whereas the underlying basement rocks gradually rise to the SE to outcrop in the Vosges Massif. As previously described, the main SE-verging thrusts form the shallowest part of the Saxothuringian retrowedge, SE of the Rhenohercynian suture zone.

5. A New Tectonic Model for the LSNB

5.1 Integration of Seismic Data Into a New Regional Structural Map

The interpreted structures are integrated at the regional scale in a new structural map of the LSNB (Figure 9). One of the main controversies in the Lorraine Basin is related to its NW structural limit and the prolongation of the SHF in NE France. This SE-dipping extensional or transtensional fault zone, bounding the Stephanian to Early Permian deposits in the Saar-Nahe Basin is considered as the main border fault controlling the development of the basin, directly to the south of the Rhenohercynian suture zone ([Henk, 1993](#); [Korsch and Schäfer, 1991, 1995](#); [Lorenz and Haneke, 2004](#); [Oncken, 1998](#); [Schneider and Romer, 2010](#); [Stollhofen, 1998](#)). Our seismic interpretations show that the Metz Fault does not correspond to the prolongation of the SHF. Instead, we show the presence of the NW-dipping Metz-Gironville thrust system, delimiting the present day extent of the syn-orogenic deposits (Figure 9). This preserved series forms a narrow strip (about 50 km wide) on top of the SE-verging Saxothuringian retrowedge that is, in the wedge-top basin (Figures 10, 11). The PAM-Merlebach and Alsting anticlines form ENE-WSW-trending thrust-related folds developed to the south of the Metz thrust zone during late Westphalian times. The out-of-sequence activation of the thrust belt induced the dissection of the PAM anticline, thus preserving only the SE forelimb of the thrust-related anticline. Although poorly constrained on the seismic profiles (see NS08 profile; Figure 7), this late dissection of the anticline can be partly attributed to the reactivation of the Metz Thrust during the Saalian compressive event (Early Permian).

The syn-orogenic sequences (Westphalian) are unconformably overlain by the synrift Stephanian-Lower Permian deposits. The latter are controlled by the overall tectonic subsidence created south of the SHF and its equivalent in the Lorraine Basin, as well as by the local reactivation of the former thrust ramps as antithetic normal faults. The Toul and Chevaumont faults delimit the Francheville extensional depocenter to the south. The Lesmenils Fault controls another depocenter directly south of the Metz-Gironville thrust

system (Figure 9). Our results furthermore argue for the existence of a significant extensional depocenter to the NW of the Metz normal fault (Figure 7). The latter is referred to as the Varennes-Vacherauville extensional depocenter in reference to the deep boreholes sampling Stephanian-Lower Permian strata. Although poorly imaged, this depocenter is suggested to be delimited to the north by the equivalent SHF major boundary fault in the Lorraine Basin (Figure 9). After the Saalian compressive phase, which induced significant rock uplift and erosion, the Francheville sub-basin appears as the thickest extensional depocenter. It includes deposits from the BSU to the Lower Permian sequence (likely up to the equivalent of the Wadern unit of the Upper Rotliegend) as suggested by the significant thickness of red beds in the Germisay borehole (1,328 m, Figure 3). The postrift sequence interpreted in the seismic profiles is likely to only correspond to the upper part of the Saxonian (i.e., Upper Rotliegend) deposits. The thickness of the synrift deposits in the Francheville sub-basin is thus of the same order of magnitude than in the Saar-Nahe region. Stephanian, Lower Rotliegend and Upper Rotliegend sequences are about 2,600, 1,700, and 1,600 m thick, respectively ([Henk, 1993](#); [Korsch and Schäfer, 1991, 1995](#); [Oncken, 1998](#); [Schneider and Romer, 2010](#); [Stollhofen, 1998](#)).

One of the main outcome of this paper is that the SHF does not correspond to the Metz fault system and the SHF has to be found further north. The northern branch of the SHF (north of the Merzig graben; Figure 9) is thus proposed to extend in the Lorraine segment of the LSNB. This point is supported by the presence of the Stephanian-Lower Permian series in the Varennes and Vacherauville wells (north of the city of Verdun; 9), as well as the recognition of a synrift depocenter NW of the Metz normal fault (see above). Such trace of the SHF also implies a progressive change of strike from N050 to N070 (from Saar-Nahe to Lorraine), following the orientation and curvature of the Rhenohercynian thrust belt in the Ardennes massif, and first-order gravimetric anomalies below the Paris Basin ([Baptiste, 2016](#); [Schintgen and Förster, 2013](#)).

The existence of diabase in the Variscan basement at the base of Vacherauville well ([Grangeon, 1953](#)) provides evidence of thrust oceanic crust of the Rhenohercynian domain, and thereby argue for the emergence of the suture zone just north of this well. Thus, the inverted Rhenohercynian suture zone along the SHF in SW Germany ([Oncken et al., 2000](#)) would be localized in a more northerly position than generally assumed. In our new structural model, the Metz Thrust is not located along the suture zone, but forms a major backthrust a few kilometers to the south of the Rhenohercynian suture zone (Figures 10 and 11).

Another major feature emphasized by our structural map is the important segmentation of the basin, which is disrupted by numerous transverse faults (Lothringen, Delme, Nancy, Comercy faults; Figure 9). There are probably other buried trans-

**A Deformed Wedge-Top Basin Inverted During the Collapse of the Variscan Belt:
The Permo-Carboniferous Lorraine Basin (NE France) — 19/28**

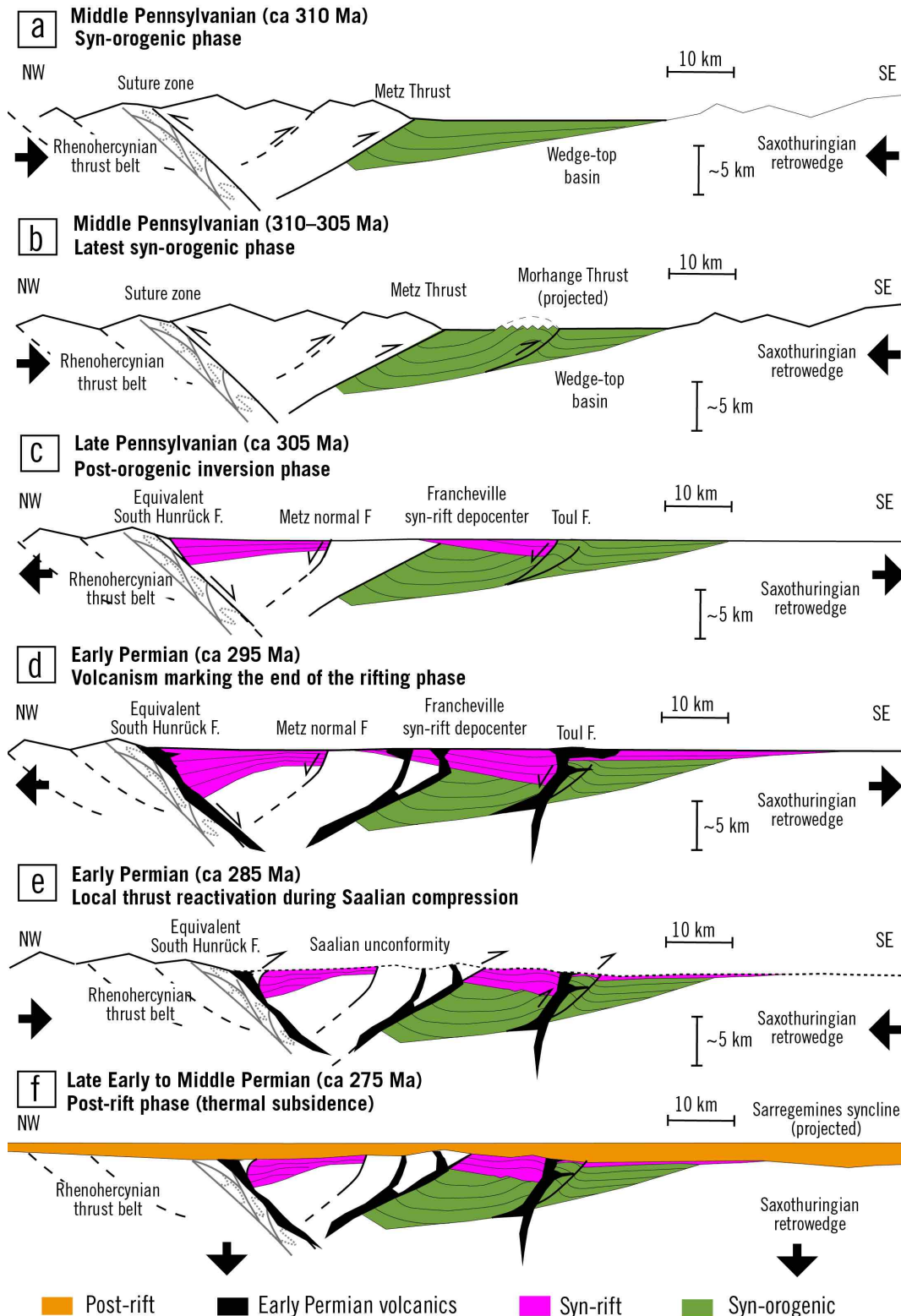


Figure 10. Schematic NW-SE cross-sections illustrating the proposed evolutionary model of the Permo-Carboniferous Lorraine Basin subdivided into 6 stages: (a) syn-orogenic basin development (Westphalian C presented here; i.e., Middle Pennsylvanian); (b) propagation of SE-verging thrusts and associated folding during Westphalian D (late Middle Pennsylvanian); (c) Post-orogenic negative tectonic inversion controlling the development of synrift depocenters (Stephanian/Late Pennsylvanian to Early Permian); (d) Early Permian synrift volcanism; (e) Local thrust reactivation during the Saalian compressional phase; (f) postrift thermal subsidence during late Early to Middle Permian times.

verse faults but they could not be imaged using the present seismic data set. These faults display a significant apparent subvertical displacement on seismic profiles inducing changes in the remnant thickness of deposits below the TPU as well as in the elevation of underlying fold-thrust structures (Figure 8). Such differential movements result in right- or left-lateral offset of the extensional depocenters and fold-thrust traces in map view. Some strike-slip component along these faults is also likely but not possible to constrain here. They clearly cut across the NE-striking thrust system (Metz, Gironville, PAM thrusts; see the EW01 longitudinal profiles, Figure 8b). Similarly, NE of the investigated area, the Morhange and Saar thrusts (Figure 9) are disrupted by the Lothringen transverse fault, displaying an apparent right-lateral offset of about 10 km (Donsimoni, 1981). Such transverse faults were also identified and well-studied in the Saar-Nahe segment of the basin where they display a regular spacing of about 10 km (Henk, 1993; Stollhofen, 1998; Stollhofen and Stanistreet, 1994). As shown by lateral syn-sedimentary variations in the Stephanian to Lower Permian series exposed in this part of the basin, these faults were proposed to be active at least during the extensional phase forming transfer zones (described as transtensional) accommodating differential subsidence and sedimentary infill (Stollhofen, 1998; Stollhofen and Stanistreet, 1994). Such transfer faults, almost perpendicular to the direction of the main normal fault system, have been frequently recognized in extensional basins and rift zones; that is, the Basin and Range (Faulds et al., 1990), Gulf of Suez rift (Moustafa, 2002), East African rift (Morley et al., 1990), Pannonian basin (Tari et al., 1992) and were the subject of extensive modeling (Liu et al., 2022; Paul and Mitra, 2013; Rodrigues et al., 2023; Schlische and Withjack, 2009). These different studies point to some variable amounts of strike-slip and normal movements along transfer faults depending on the obliquity of the extension direction. In the absence of detailed kinematical analysis of these transverse faults in the LSNB, it is impossible to conclude on the way both systems of faults (i.e., transverse and thrust-parallel) interact during the basin development.

Based on coal mining investigations, the Metz Thrust is assumed to be displaced by transverse faults, giving rise to complex geometry of the thrust system limiting the syn-orogenic deposits. Such fault pattern is consistent with the structural model proposed in Saar-Nahe considering that the transverse faults connect to the SHF (Henk, 1993; Stollhofen, 1998). The prolongation of the Metz Thrust in the Saar-Nahe domain is buried below the postrift succession (Upper Rotliegend); it is usually assumed to join the southern branch of the SHF but the displacement on this thrust may also fade eastward, shortening being transferred onto another major thrust of the basin, possibly the Saar Thrust (Figure 9).

The Saarbrücken anticline (Figure 9) is not imaged by our seismic data. However, as previously discussed for the

Alsting anticline and also corroborated by vitrinite reflectance data (Hertle and Littke, 2000), two superimposed shortening phases are likely to explain the present day geometry and the involvement of Stephanian strata into the Saar thrust structure, that is, the late Variscan syn-collisional phase during late Westphalian and the Saalian phase during late Early Permian time.

5.2 Structural Development of the Permo-Carboniferous LSNB

The structural development of the Permo-Carboniferous Lorraine basin is depicted in a series of schematic cross-sections (Figure 10) summarizing the main tectonic features observed in the seismic profiles. The main evolutionary stages of basin development are illustrated here: (a) an early stage of basin development during Westphalian C (Middle Pennsylvanian); (b) a late Westphalian stage (late Middle Pennsylvanian) highlighting the propagation of thrusting and folding into the basin; (c) the Stephanian (Late Pennsylvanian)-Early Permian extension (i.e., Lower Rotliegend; ca. 300 Ma), characterized by the reactivation of the Rhenohercynian suture zone (SHF and equivalent in Lorraine) and of the NW-dipping thrusts into the basin (i.e., Toul and Metz normal faults); (d) the Early Permian volcanic activity (ca. 295 Ma) marking the end of the extensional phase; (e) a late Early Permian stage (ca. 285 Ma) showing the local reactivation of both thrusts and normal faults during the Saalian compression; (f) a final late Early to Middle Permian stage (Upper Rotliegend; ca. 275 Ma) associated with the onset of postrift thermal subsidence and sedimentation above the post-Saalian erosional surface. In this new model, it is proposed that the basin was initiated during Early Pennsylvanian (Late Namurian, ca. 320 Ma) at the foot of the reliefs created by the most internal backthrusts of the Saxothuringian retrowedge. The latter are suggested to root down onto the SE-dipping Rhenohercynian suture zone and progressively propagate toward the orogenic basin (Figure 10). Up to the late Middle Pennsylvanian (late Westphalian, ca. 305 Ma), the syn-orogenic trough was fed by the products of erosion from the Rhenohercynian prowedge and Saxothuringian retrowedge. This trough moved progressively SE-ward with the propagation of the retrowedge as shown by onlap of the sediment infill onto the underlying substratum (probably of Devonian age). It is rather difficult to have a precise view of the kinematics of the Metz Thrust that delimits the Westphalian units to the NW but unusually thick conglomeratic deposits (at least 400 m thick) within the Westphalian C sequences in the Chaumont well (Izart et al., 2005), in the direct footwall of the Metz-Gironville thrust system, support the fact that it was emergent at least by stage a (Figure 10).

During late Middle Pennsylvanian (stage b; Figure 10), deformation progressively migrated toward the SE, with development of intrabasinal folds and thrusts (e.g., Morhange thrust) as documented by growth strata in the forelimbs of

these anticlines. The basin was mainly supplied by rivers draining the surrounding high-altitude massifs; at least 3 km above sea level (Hillenbrand and Williams, 2022). The eroded anticlines demonstrate that rock uplift was also generated at that time within the basin, the eroded material being recycled during syn- and early post-orogenic stages. Such scenario of syn-orogenic deformation on top of the retrowedge is notably consistent with the timing of deformation in the Rhenohercynian foredeep, as shown within the foreland molassic coal basin of Northern France-Southern Belgium (Laurent et al., 2021). Such kinematical coherency supports a first-order coupling of both hinterland and foreland of the Variscan belt during the collision process as suggested by sand-box modeling experiments (Hoth et al., 2008). Top-retrowedge syn-orogenic basin developing at the back of the suture zone (Figure 11) is not a common tectonic feature within orogenic belts but the Tertiary Piedmont basin at the southeastern border of the Western Alps internal zone is considered as an analog (Bertotti et al., 2006; Capponi et al., 2009; Carrapa et al., 2004; Carrapa and Garcia-Castellanos, 2005; Garzanti and Malusà, 2008; Maino et al., 2013; Roure et al., 1990).

Another major outcome of this study is the evidence of a negative tectonic inversion process, with Stephanian synrift strata deposited unconformably above the deformed Westphalian basin. The synrift depocenters are specifically located along the former crests and backlimb of thrust-related anticlines. The former late Westphalian structural highs become structural lows, localizing the main depocenters, thus characterizing the negative tectonic inversion process. This tectonic inversion involves the reactivation of Westphalian thrust ramps and underlying decollements as normal faults and extensional detachments, respectively (stage c; Figure 10). Such a change in stress regime across the basin is responsible for the creation of a major unconformity (BSU) between the Westphalian and Stephanian strata. The BSU marks the end of the major collision stage and the onset of the post-orogenic extensional phase (i.e., tectonic collapse stage). The sedimentary response to such a major change in regional kinematics was associated with the reorganization of river systems, leading to the basin-wide deposition of the Holz conglomerates and a possible change in the main sediment source from north to south (Schäfer, 1989). Such a general depositional pattern suggests that rock uplift was particularly localized in the prowedge zone (Rhenohercynian thrust belt; Figure 11) during the syn-orogenic phase, and was subsequently more widely distributed across the orogen during the post-orogenic extensional phase, implying river supply from different sources. The Metz border thrust remained a structural high during the post-orogenic phase, but a Stephanian depocenter developed further north and south (i.e., Varennes-Vacherauville and Francheville depocenters respectively). The SHF, which reactivates at depth the Rhenohercynian suture, is suggested to be located north of the Verdun area (Figure 9). The extension-related basin is about 100 km wide, covering a

larger area than the initial syn-orogenic trough.

The synrift infill in the western part of the Lorraine basin reaches up to about 4.5 km. In addition to the well-defined Stephanian sequence, the synrift infill may also include some Lower Permian deposits, known as the Autunian series in late Variscan French basins (e.g. Becq-Giraudon et al., 1995, 1996; Burg et al., 1994), and likely equivalent to the Lower Rotliegend unit in Germany (stage d; Figure 10). It would thus imply an upper age of the synrift series at about 290 Ma, as documented by the age of the volcanic intrusions in Saar-Nahe (von Seckendorff et al., 2004). Although not precisely dated, the post-orogenic volcanism in Lorraine would also mark the end of the extensional phase in the basin. As observed in seismic profiles and represented in Figure 10, volcanic extrusions are preferentially located in the vicinity of major faults (hangingwall of the Metz thrust, footwall of the Toul and Chevaumont faults) suggesting that the faults represent preferential magma pathways.

Based on detailed petrological studies, a mixed crustal and mantle source is inferred for intermediate type volcanics in the Saar-Nahe segment of the LSNB (Arz, 1996; von Seckendorff et al., 2004). Magmatism would be driven by underplating of mantle-derived melts and associated partial melting of the lower crust. Such extensive involvement of mantle melting in the syn- to post-orogenic magmatic suites within the Armorican-Saxothuringian-Moldanubian units forming the upper plate of the Rhenohercynian subducted slab, has been widely interpreted to be the result of lithospheric delamination and removal of the Variscan orogenic roots (Averbuch and Piromallo, 2012; Caroff et al., 2021; Finger et al., 2009; Guillot et al., 2020; Henk, 1993; Janoušek and Holub, 2007; Kubínová et al., 2017; Laurent et al., 2017). The synrift depocenters (Stephanian-Early Permian) driven by negative inversion of the Variscan thrusts, are proposed to represent another record of such process of removal of the lithospheric orogenic roots.

Post-orogenic events also include the subsequent positive tectonic inversion of the basin during the Saalian compressional phase (stage e; Figure 10); this event is considered to be late Early Permian in age (Donsimoni, 1981; Guerrier and Pruvost, 1965; Kneuper, 1976; Pruvost, 1956; Prost and Becq-Giraudon, 1989) and, thus occurred shortly after the extensive magmatic event. This deformation event is poorly expressed in the study area. Apart from the significant regional uplift and erosion of the basin, it is evidenced by locally folded and thrusting Stephanian series (Saar and Morhange thrusts; Figure 9). This probably short compressional phase is poorly constrained in terms of age and amount of deformation. The maximum amount of denudation related to the Saalian shortening in the Lorraine domain is estimated at 1,200 m (Izart et al., 2016) while a maximum of 3,200 m of sediments have been suggested to have been eroded in Saar-Nahe Basin (Her-

tle and Littke, 2000).

The postrift sequence (Upper Rotliegend in Saar-Nahe) consists of red beds deposited unconformably above the strongly irregular Saalian erosion surface (stage f; Figure 10). Maximum thickness of the postrift series is preferentially localized on the previous lows inherited from the Saalian deformation. This sequence is considered to have developed under a general thermal subsidence regime, due to lithospheric cooling following the extensive magmatism (Stollhofen, 1998; von Seckendorff et al., 2004). Within this general scenario, it is interesting to note that the base of this sequence would correspond to the superposition of two regional unconformities that is, the post-Saalian unconformity and the postrift unconformity. As classically observed for postrift sequences, these deposits overstep the initial borders of the basin both northward and southward onto the Variscan basement. The postrift sequence represents a relatively thin interval (less than 500 m thick) locally preserved below the TPU with a lenticular geometry. The subsequent long-term (Triassic to Upper Cretaceous) thermal subsidence of the lithosphere led to the formation of the Paris Basin as a post-Variscan sag basin (Averbuch and Piromallo, 2012; Prijac et al., 2000; Robin et al., 2003).

6. Conclusions

The analysis of significant data set of reprocessed seismic profiles (438 km) in NE France provides a new structural framework and geodynamic evolution of the Permo-Carboniferous Lorraine Basin. This basin, which forms the westernmost part of the major late Variscan intramountain LSNB, provides a record of the geodynamic processes active at the transition between the collisional and post-orogenic tectonic collapse stages. The Lorraine Basin originated as a Late Namurian-Westphalian (Early-Middle Pennsylvanian) syn-orogenic depocenter developed in a wedge-top position upon the syn-collisional Saxothuringian retro-wedge. Thrusts propagated toward the SE during sedimentation of the Upper Westphalian strata (mostly Westphalian D; late Middle Pennsylvanian) as emphasized by growth structures in the forelimbs of the folds.

After a short period of subaerial erosion of the thrust-related anticlines, which resulted in a pronounced angular unconformity, subsidence resumed from Stephanian (Late Pennsylvanian) to late Early Permian times. This tectonic phase is proposed here to be due to the extensional (or transtensional) reactivation of the suture zone (SHF) and SE-verging internal thrusts of the basin featuring a major post-orogenic negative tectonic inversion. This event is at the origin of the overall half-graben structure of the basin covering a wider area than during the initial syn-orogenic stage.

The seismic profiles highlight the strongly segmented character of the basin, inverted extensional depocenters being transferred and controlled along strike by transverse NNW-SSE striking faults. In this regard, the investigated seis-

mic profiles document the existence of a major depocenter in the western end of the Lorraine Basin. The late synrift phase (i.e., Early Permian) is marked by volcanic extrusions along some pre-existing major fault zones (the Metz and Toul-Chevaumont fault zones). Such volcanic activity at the end of the synrift phase is rapidly followed by local reactivation of both thrusts and normal faults, inducing a general uplift of the basin (Saalian compression). This phase is poorly expressed in the Lorraine segment of the basin while it likely accounts for a more significant part of shortening and overall deformation in the Saar-Nahe segment. Finally, the postrift sequence (Upper Rotliegend; late Early Permian), controlled by thermal subsidence, developed above the post-Saalian erosional surface.

An important result is the documentation of a major SE-directed backthrust system (the Metz Thrust) delimiting the northern border of the syn-orogenic basin. This fault zone does not correspond to the direct prolongation of the SHF as it was currently interpreted in the past. The SHF corresponds to the inverted Rhenohercynian suture zone, and such equivalent post-orogenic structure in the Lorraine Basin has to be found further north; that is, north of the Varennes-Vacherauville depocenter. The distinction between syn- and post-orogenic structures is an important outcome of this paper. The complex geometry due to inversion tectonics and basin segmentation gave rise to misleading interpretations in the past, especially concerning the location and nature of the main border fault in Lorraine and the construction of a coherent tectonic history between NE France and SW Germany.

The Late Carboniferous negative tectonic inversion along the Rhenohercynian suture zone and the associated collapse of Variscan belt are proposed to result from the removal of the orogenic root at the end of the collision. The associated upwelling of hot asthenospheric material is likely to have driven the intense magmatic activity observed in the basin at the end of the synrift phase. The resultant thermal anomaly is suggested to form the main trigger for the subsequent thermal subsidence of the Late Permian-Mesozoic Paris Basin (i.e., a post-delamination sag basin). The late evolution of the Variscan orogenic system thus appears as a complex transition phase where both compression and extension can be recorded in the same area over a short period (less than 10 Myr). Further absolute dating within the thick continental series of the LSNB is necessary to provide basin scale correlations and better definition of processes involved in the tectonic collapse of this major orogenic belt.

Data Availability Statement

According to French laws, the field seismic data are publicly available at <http://www.minergies.fr/fr>. The reprocessed seismic data (SEG-Y) used in this paper belong to the BRGM, so they can be released only with a formal agreement with the BRGM.

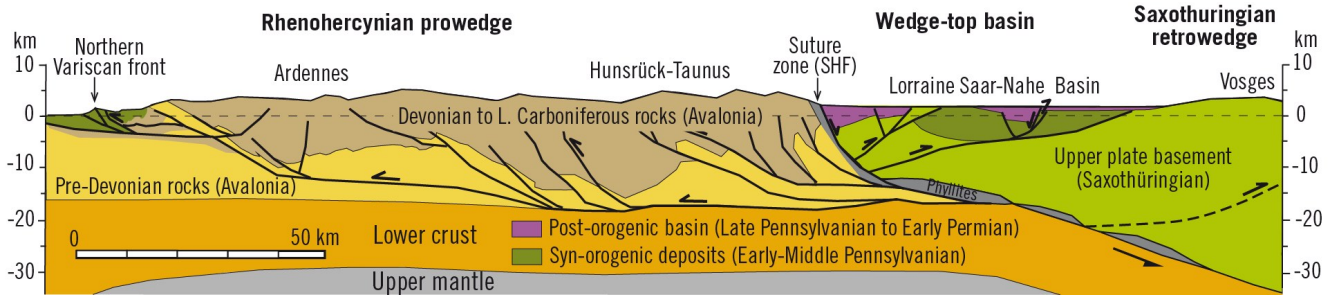


Figure 11. Synthetic crustal cross-section representing the Variscan orogenic belt in the Rhenohercynian suture zone area at about 300–295 Ma, that is, during the post-orogenic extensional collapse stage. Note the position of the Namurian-Westphalian (Early-Middle Pennsylvanian) depocenter (dark green) forming a syn-orogenic wedge-top basin upon the Saxothuringian retro-wedge, directly SE of the Rhenohercynian suture. The post-orogenic Stephanian (Late Pennsylvanian)-Lower Permian depocenters (purple) result from tectonic subsidence generated by extensional reactivation of the suture zone (South-Hunsrück Fault) and of intra-basin thrusts generated formerly during the latest increments of the collisional deformation (late Middle Pennsylvanian). The geometry of the Rhenohercynian prowedge is based on the balanced crustal cross-section of (Oncken et al., 2000).

Acknowledgments

This study forms part of a collaborative project between the BRGM, the University of Lille, the University of Lorraine and the CNRS, and benefitted from funds from the different institutes. Reprocessing of the seismic profiles was mainly funded by the BRGM. L. Beccalotto thanks the Georesources Division of the BRGM for supporting this work. This study also benefitted from the support of the INSU-SYSTER program of the CNRS (DELAM project, PI O. Averbuch). The 3D integration of seismic profiles was held during the post-doctoral work of R. Hemelsdaël funded by BRGM and the 'Lorraine Université d'Excellence' research initiative (DEEP-SURF project, reference ANR-15-IDEX-04-LUE). The authors acknowledge M. Ford for her careful reading of the manuscript, improvement of the English style and scientific comments. J.W. Schneider, A. Schäfer and S. Oplustil are also greatly thanked for fruitful discussions related to the geological evolution of the LSNB. We thank the associate editor, Djordje Grujic, as well as Piotr Krzywiec and an anonymous reviewer, for their valuable comments to improve the previous versions of this article.

References

- Alpern, B., Choffé, M., Lachkar, G., and Liabeuf, J.-J. (1969). Synthèse des zonations palynologiques des bassins houillers de Lorraine et de Sarre. *Revue de Micropaléontologie*, 4:217–221.
- Anderle, H. (1987). The evolution of the South Hunsrück and Taunus Border zone. *Tectonophysics*, 137(1-4):101–114.
- Anderle, H., Franke, W., and Schwab, M. (1995). Stratigraphy. In *Pre-Permian Geology of Central and Eastern Europe*, pages 99–107. Springer Berlin Heidelberg, Berlin, Heidelberg.
- Aretz, M., Herbig, H., Wang, X., Gradstein, F., Agterberg, F., and Ogg, J. (2020). The Carboniferous Period. In *Geologic Time Scale 2020*, pages 811–874. Elsevier.
- Arz, C. (1996). Origin and petrogenesis of igneous rocks from the Saar-Nahe-Basin (SW-Germany): Isotope, trace element and mineral chemistry. *PhD Thesis, Julius-Maximilians-Universität, Würzburg*.
- Averbuch, O., Frizon de Lamotte, D., and Kissel, C. (1992). Magnetic fabric as a structural indicator of the deformation path within a fold-thrust structure: a test case from the Corbières (NE Pyrenees, France). *Journal of Structural Geology*, 14(4):461–474.
- Averbuch, O. and Piromallo, C. (2012). Is there a remnant Variscan subducted slab in the mantle beneath the Paris basin? Implications for the late Variscan lithospheric delamination process and the Paris basin formation. *Tectonophysics*, 558-559:70–83.
- Baptiste, J. (2016). Cartographie structurale et lithologique du substratum du Bassin parisien et sa place dans la chaîne varisque de l'Europe de l'Ouest: approches combinées géophysiques, pétrophysiques, géochronologiques et modélisations 2D. *Thèse de doctorat, Université d'Orléans*, page 374p.
- Beccalotto, L., Capar, L., Serrano, O., and Marc, S. (2015). Structural evolution and sedimentary record of the Stephano-Permian basins occurring beneath the Mesozoic sedimentary cover in the southwestern Paris basin (France). *Bulletin de la Société Géologique de France*, 186(6):429–450.
- Becker, A. and Schäfer, A. (2021). Evolution of the Saar-Nahe Basin in the late Palaeozoic. *Jahresberichte und Mitteilungen des Oberrheinischen Geologischen Vereins*, 103:211–233.

- Becq-Giraudon, J.-F., Mercier, D., and Jacquemin, H. (1995). Faut-il rassembler le Stéphaniens supérieur et l'Autunien (Paléozoïque supérieur continental) en une seule entité lithostratigraphique? *Géologie de la France*, (2):17–24.
- Becq-Giraudon, J.-F., Montenat, C., and Van Den Driessche, J. (1996). Hercynian high-altitude phenomena in the French Massif Central: tectonic implications. *Palaeogeography, Palaeoclimatology, Palaeoecology*, 122(1-4):227–241.
- Bertotti, G., Mosca, P., Juez, J., Polino, R., and Dunai, T. (2006). Oligocene to Present kilometres scale subsidence and exhumation of the Ligurian Alps and the Tertiary Piedmont Basin (NW Italy) revealed by apatite (U-Th)/He thermochronology: correlation with regional tectonics. *Terra Nova*, 18(1):18–25.
- Bertrand, P. (1930). *Bassin Houiller de la Sarre et de la Lorraine. Flore Fossile. Fascicule 1. Neuropteridees*. Alexander Doweld.
- Bond, C. E., Lunn, R., Shipton, Z., and Lunn, A. (2012). What makes an expert effective at interpreting seismic images? *Geology*, 40(1):75–78.
- Bouroz, A., Knight, J. A., Wagner, R. H., and Winkler Prins, C. F. (1972). Sur la limite Westphalien-Stéphaniens et sur les subdivisions du Stéphaniens inférieur sensu lato (Rapport du groupe de travail sur le Stéphaniens). *Compte Rendu 7ème Congrès Carbonifère. Krefeld*, 1:241–261.
- Brun, J., Gutscher, M.-A., and ecors teams, D. (1992). Deep crustal structure of the Rhine Graben from deKorp-ecors seismic reflection data: A summary. *Tectonophysics*, 208(1-3):139–147.
- Burg, J.-P., van den Driessche, J., and Brun, J.-P. (1994). Syn- to post-thickening extension in the Variscan Belt of Western Europe: modes and structural consequences. *Géologie de la France*, (3):33–51.
- Burger, K., Hess, J. C., and Lippolt, H. J. (1997). *Tephrochronologie mit Kaolin-Kohlentonsteinen: Mittel zur Korrelation paralischer und limnischer Ablagerungen des Oberkarbons*. Schweizerbart.
- Capponi, G., Crispini, L., Federico, L., Piazza, M., and Fabbri, B. (2009). Late Alpine tectonics in the Ligurian Alps: constraints from the Tertiary Piedmont Basin conglomerates. *Geological Journal*, 44(2):211–224.
- Caroff, M., Barrat, J.-A., and Le Gall, B. (2021). Kersantites and associated intrusives from the type locality (Kersanton), Variscan Belt of Western Armorica (France). *Gondwana Research*, 98:46–62.
- Carrapa, B., Di Giulio, A., and Wijbrans, J. (2004). The early stages of the Alpine collision: an image derived from the upper Eocene–lower Oligocene record in the Alps–Apennines junction area. *Sedimentary Geology*, 171(1-4):181–203.
- Carrapa, B. and Garcia-Castellanos, D. (2005). Western Alpine back-thrusting as subsidence mechanism in the Tertiary Piedmont Basin (Western Po Plain, NW Italy). *Tectonophysics*, 406(3-4):197–212.
- Chantraine, J., Autran, A., Cavelier, C., Alabouvette, B., Barféty, J. C., Cecca, F., Clozier, L., Debrand-Passard, S., Dubreuilh, J., and Feybesse, J. L. (2003). Carte géologique de la France à 1/1 000 000. *BRGM Orléans édition*, 6ème édit.
- Courel, L., Donsimoni, M., and Mercier, D. (1986). La place du charbon dans la dynamique des systèmes sédimentaires des bassins houillers intramontagneux. *Société Géologique de France*, 149:37–50.
- Debrand-Passard, S. (1980). Synthèse géologique du bassin de Paris - Atlas. *Mémoire BRGM 102*, 2.
- Delmas, J., Houel, P., and Vially, R. (2002). Paris Basin Petroleum Potential. *IFP Rapport d'évaluation Pétrolière*, page 179p.
- Dewey, J. F. (1988). Extensional collapse of orogens. *Tectonics*, 7(6):1123–1139.
- Donsimoni, M. (1981). Le bassin houiller lorrain. Synthèse géologique. *Mémoire BRGM Orléans*, 117:102 p.
- Edel, J.-B. and Schulmann, K. (2009). Geophysical constraints and model of the “Saxothuringian and Rhenohercynian subductions – magmatic arc system” in NE France and SW Germany. *Bulletin de la Société Géologique de France*, 180(6):545–558.
- Edel, J.-B., Schulmann, K., Skrzypek, E., and Cocherie, A. (2013). Tectonic evolution of the European Variscan belt constrained by palaeomagnetic, structural and anisotropy of magnetic susceptibility data from the Northern Vosges magmatic arc (eastern France). *Journal of the Geological Society*, 170(5):785–804.
- Engel, W. (1988). Neue Erkenntnisse zum geologischen Werdegang des Saarkarbons. *Doc. Nat.*, 44:8–22.
- Faulds, J. E., Geissman, J. W., and Mawer, C. K. (1990). Structural development of a major extensional accommodation zone in the Basin and Range Province, northwestern Arizona and southern Nevada; Implications for kinematic models of continental extension. *Basin and range extensional tectonics near the latitude of Las Vegas, Nevada: Geological Society of America Memoir*, 176:37–76.
- Faure, M. (1995). Late orogenic Carboniferous extensions in the Variscan French Massif Central. *Tectonics*, 14(1):132–153.
- Finger, F., Gerdes, A., René, M., and Riegler, G. (2009). The Saxo-Danubian Granite Belt: magmatic response to post-collisional delamination of mantle lithosphere below

- the southwestern sector of the Bohemian Massif (Variscan orogen). *Geologica Carpathica*, 60(3):205–212.
- Fleck, S., Michels, R., Izart, A., Elie, M., and Landais, P. (2001). Palaeoenvironmental assessment of Westphalian fluvio-lacustrine deposits of Lorraine (France) using a combination of organic geochemistry and sedimentology. *International Journal of Coal Geology*, 48(1-2):65–88.
- Franke, W. (2000). The mid-European segment of the Variscides: tectonostratigraphic units, terrane boundaries and plate tectonic evolution. *Geological Society, London, Special Publications*, 179(1):35–61.
- Franke, W. (2014). Topography of the Variscan orogen in Europe: failed–not collapsed. *International Journal of Earth Sciences*, 103(5):1471–1499.
- Friedl, E. and Siviard, E. (1932). Bassin houiller de la Sarre et de la Lorraine. *Atlas. Études des Gîtes Minéraux de la France. Paris*.
- Gardner, G. H. F., Gardner, L. W., and Gregory, A. R. (1974). Formation velocity and density — The diagnostic basics for stratigraphic traps. *GEOPHYSICS*, 39(6):770–780.
- Garzanti, E. and Malusà, M. G. (2008). The Oligocene Alps: Domal unroofing and drainage development during early orogenic growth. *Earth and Planetary Science Letters*, 268(3-4):487–500.
- Gawthorpe, R. L., Sharp, I., Underhill, J. R., and Gupta, S. (1997). Linked sequence stratigraphic and structural evolution of propagating normal faults. *Geology*, 25(9):795.
- Gély, J.-P. and Hanot, F. (2014). *Le bassin parisien: un nouveau regard sur la géologie*. Association des géologues du Bassin de Paris.
- Göğüş, O. H. and Pysklywec, R. N. (2008). Mantle lithosphere delamination driving plateau uplift and synconvergent extension in eastern Anatolia. *Geology*, 36(9):723.
- Göğüş, O. H., Pysklywec, R. N., and Faccenna, C. (2016). Postcollisional lithospheric evolution of the Southeast Carpathians: Comparison of geodynamical models and observations. *Tectonics*, 35(5):1205–1224.
- Grangeon (1953). Sondage de Vacherauville (Meuse), Observations sur le Paléozoïque et le socle anté-Carbonifère. *Rapport BRGM*, page 15p.
- Guerrier, R. and Pruvost, P. (1965). La limite septentrionale du bassin houiller de la Lorraine. *Comptes Rendu de Académie des Sciences de Paris*, 261:5349–5553.
- Guillot, F., Averbuch, O., Dubois, M., Durand, C., Lanari, P., and Gauthier, A. (2020). Zircon age of vaugnerite intrusives from the Central and Southern Vosges crystalline massif (E France): contribution to the geodynamics of the European Variscan belt. *BSGF - Earth Sciences Bulletin*, 191:26.
- Henk, A. (1992). Mächtigkeit und Alter der erodierten Sedimente im Saar-Nahe-Becken (SW-Deutschland). *Geologische Rundschau*, 81(2):323–331.
- Henk, A. (1993). Late orogenic Basin evolution in the Variscan internides: the Saar-Nahe Basin, southwest Germany. *Tectonophysics*, 223(3-4):273–290.
- Henk, A. (2000). Foreland-directed lower-crustal flow and its implications for the exhumation of high-pressure-high-temperature rocks. *Geological Society, London, Special Publications*, 179(1):355–368.
- Hertle, M. and Littke, R. (2000). Coalification pattern and thermal modelling of the Permo-Carboniferous Saar Basin (SW-Germany). *International Journal of Coal Geology*, 42(4):273–296.
- Hillenbrand, I. W. and Williams, M. L. (2022). Geochemical Evidence for Diachronous Uplift and Synchronous Collapse of the High Elevation Variscan Hinterland. *Geophysical Research Letters*, 49(21):e2022GL100435.
- Hoth, S., Kukowski, N., and Oncken, O. (2008). Distant effects in bivergent orogenic belts — How retro-wedge erosion triggers resource formation in pro-foreland basins. *Earth and Planetary Science Letters*, 273(1-2):28–37.
- Houseman, G. A., McKenzie, D. P., and Molnar, P. (1981). Convective instability of a thickened boundary layer and its relevance for the thermal evolution of continental convergent belts. *Journal of Geophysical Research: Solid Earth*, 86(B7):6115–6132.
- Izart, A., Barbarand, J., Michels, R., and Privalov, V. (2016). Modelling of the thermal history of the Carboniferous Lorraine Coal Basin: Consequences for coal bed methane. *International Journal of Coal Geology*, 168:253–274.
- Izart, A., Palain, C., Malatre, F., Fleck, S., and Michels, R. (2005). Palaeoenvironments, paleoclimates and sequences of Westphalian deposits of Lorraine coal basin (Upper Carboniferous, NE France). *Bulletin de la Société Géologique de France*, 176(3):301–315.
- Janecke, S. U., Vandenburg, C. J., and Blankenau, J. J. (1998). Geometry, mechanisms and significance of extensional folds from examples in the Rocky Mountain Basin and Range province, U.S.A. *Journal of Structural Geology*, 20(7):841–856.
- Janoušek, V. and Holub, F. V. (2007). The causal link between HP-HT metamorphism and ultrapotassic magmatism in collisional orogens: case study from the Moldanubian Zone of the Bohemian Massif. *Proceedings of the Geologists' Association*, 118(1):75–86.
- Jolivet, L., Lecomte, E., Huet, B., Denèle, Y., Lacombe, O., Labrousse, L., Le Pourhiet, L., and Mehl, C. (2010). The

- North Cycladic Detachment System. *Earth and Planetary Science Letters*, 289(1-2):87–104.
- Kneuper, G. (1976). Regional Geologische Folgerungen aus der Bohrung Saar-1. 27:417–428.
- Knight, J. A. and Álvarez-Vázquez, C. (2021). A summary of upper Pennsylvanian regional substages defined in NW Spain – the chronostratigraphic legacy of Robert H. Wagner. *Newsletters on Stratigraphy*, 54(3):275–300.
- Königer, S. and Lorenz, V. (2002). Geochemistry, tectonomagmatic origin and chemical correlation of altered Carboniferous–Permian fallout ash tuffs in southwestern Germany. *Geological Magazine*, 139(05).
- Königer, S., Lorenz, V., Stollhofen, H., and Armstrong, R. (2002). Origin, age and stratigraphic significance of distal fallout ash tuffs from the Carboniferous-Permian continental Saar-Nahe Basin (SW Germany). *International Journal of Earth Sciences*, 91(2):341–356.
- Korsch, R. and Schäfer, A. (1991). Geological interpretation of DEKORP deep seismic reflection profiles 1C and 9N across the variscan Saar-Nahe Basin southwest Germany. *Tectonophysics*, 191(1-2):127–146.
- Korsch, R. and Schäfer, A. (1995). The Permo-Carboniferous Saar-Nahe Basin, south-west Germany and north-east France: basin formation and deformation in a strike-slip regime. *Geologische Rundschau*, 84(2):293–318.
- Kubínová, Š., Faryad, S. W., Verner, K., Schmitz, M., and Holub, F. (2017). Ultrapotassic dykes in the Moldanubian Zone and their significance for understanding of the post-collisional mantle dynamics during Variscan orogeny in the Bohemian Massif. *Lithos*, 272-273:205–221.
- Laurent, A., Averbuch, O., Beccaletto, L., Graveleau, F., Lacquement, F., Capar, L., and Marc, S. (2021). 3-D Structure of the Variscan Thrust Front in Northern France: New Insights From Seismic Reflection Profiles. *Tectonics*, 40(7):e2020TC006642.
- Laurent, O., Couzinié, S., Zeh, A., Vanderhaeghe, O., Moyaen, J.-F., Villaros, A., Gardien, V., and Chelle-Michou, C. (2017). Protracted, coeval crust and mantle melting during Variscan late-orogenic evolution: U–Pb dating in the eastern French Massif Central. *International Journal of Earth Sciences*, 106(2):421–451.
- Laveine (1974). Précisions sur la répartition stratigraphique des principales espèces végétales du Carbonifère supérieur de Lorraine. *Comptes Rendu de Académie des Sciences de Paris*, 278(D):851–854.
- Le Pourhiet, L., Burov, E., and Moretti, I. (2004). Rifting through a stack of inhomogeneous thrusts (the dipping pie concept). *Tectonics*, 23:TC4005.
- Le Roux, J. (2000). Structuration of the north-eastern Paris Basin. *Bulletin d'information des géologues du bassin de Paris*, 37(4):13–34.
- Legrand, X., Soula, J.-C., and Rolando, J.-P. (1991). Effet d'une inversion tectonique négative dans le Sud du Massif Central-français: la structure roll-over du bassin permien de Saint-Affrique. *Comptes rendus de l'Académie des sciences. Série 2, Mécanique, Physique, Chimie, Sciences de l'univers, Sciences de la Terre*, 312(9):1021–1026.
- Liu, J., Yang, H., Xu, K., Wang, Z., Liu, X., Cui, L., Zhang, G., and Liu, Y. (2022). Genetic mechanism of transfer zones in rift basins: Insights from geomechanical models. *GSA Bulletin*, 134(9-10):2436–2452.
- Lorenz, V. and Haneke, J. (2004). Relationship between diatremes, dykes, sills, laccoliths, intrusive-extrusive domes, lava flows, and tephra deposits with unconsolidated water-saturated sediments in the late Variscan intermontane Saar-Nahe Basin, SW Germany. *Geological Society, London, Special Publications*, 234(1):75–124.
- Lucas, S. G., Schneider, J., Nikolaeva, S., and Wang, X. (2022). The Carboniferous chronostratigraphic scale: history, status and prospectus. *Geological Society, London, Special Publications*, 512(1):19–48.
- Maino, M., Decarlis, A., Felletti, F., and Seno, S. (2013). Tectono-sedimentary evolution of the Tertiary Piedmont Basin (NW Italy) within the Oligo-Miocene central Mediterranean geodynamics. *Tectonics*, 32(3):593–619.
- Malavieille, J., Guihot, P., Costa, S., Lardeaux, J., and Gardien, V. (1990). Collapse of the thickened Variscan crust in the French Massif Central: Mont Pilat extensional shear zone and St. Etienne Late Carboniferous basin. *Tectonophysics*, 177(1-3):139–149.
- Massonne, H.-J. (1995). Metamorphic Evolution. In *Pre-Permian Geology of Central and Eastern Europe*, pages 132–137. Springer Berlin Heidelberg, Berlin, Heidelberg.
- McCann, T., Pascal, C., Timmerman, M., Krzywiec, P., López-Gómez, J., Wetzel, L., Krawczyk, C., Rieke, H., and Lamarche, J. (2006). Post-Variscan (end Carboniferous–Early Permian) basin evolution in Western and Central Europe. *Geological Society, London, Memoirs*, 32(1):355–388.
- McClay, K. (1990). Extensional fault systems in sedimentary basins: a review of analogue model studies. *Marine and Petroleum Geology*, 7(3):206–233.
- Ménard, G. and Molnar, P. (1988). Collapse of a Hercynian Tibetan Plateau into a late Palaeozoic European Basin and Range province. *Nature*, 334(6179):235–237.

- Minguely, B., Averbuch, O., Patin, M., Rolin, D., Hanot, F., and Bergerat, F. (2010). Inversion tectonics at the northern margin of the Paris basin (northern France): new evidence from seismic profiles and boreholes interpolation in the Artois area. *Bulletin de la Société Géologique de France*, 181(5):429–442.
- Mohapatra, G. K. and Johnson, R. A. (1998). Localization of listric faults at thrust fault ramps beneath the Great Salt Lake Basin, Utah: Evidence from seismic imaging and finite element modeling. *Journal of Geophysical Research: Solid Earth*, 103(B5):10047–10063.
- Morency, C., Doin, M.-P., and Dumoulin, C. (2002). Convective destabilization of a thickened continental lithosphere. *Earth and Planetary Science Letters*, 202(2):303–320.
- Morley, C., Nelson, A., Patton, T., and Munn, S. (1990). Transfer Zones in the East African Rift System and Their Relevance to Hydrocarbon Exploration in Rifts (1). *AAPG Bulletin*, 74:1234–1253.
- Moustafa, A. (2002). Controls on the geometry of transfer zones in the Suez rift and northwest Red Sea: Implications for the structural geometry of rift systems. *AAPG Bulletin*, 86:979–1002.
- Oncken, O. (1997). Transformation of a magmatic arc and an orogenic root during oblique collision and its consequences for the evolution of the European Variscides (Mid-German Crystalline Rise). *Geologische Rundschau*, 86(1):2–20.
- Oncken, O. (1998). Orogenic mass transfer and reflection seismic patterns — evidence from DEKORP sections across the European Variscides (central Germany). *Tectonophysics*, 286(1-4):47–61.
- Oncken, O., Plesch, A., Weber, J., Ricken, W., and Schrader, S. (2000). Passive margin detachment during arc-continent collision (Central European Variscides). *Geological Society, London, Special Publications*, 179(1):199–216.
- Ouzgaït, M., Averbuch, O., Vendeville, B., Zuo, X., and Minguely, B. (2010). The negative tectonic inversion of thrust faults: Insights from seismic sections along the Northern France Variscan thrust front and analogue modelling experiments. *GeoMod2010, Lisbon, Extended abstract*, 27(19):95–98.
- Paul, D. and Mitra, S. (2013). Experimental models of transfer zones in rift systems. *AAPG Bulletin*, 97(5):759–780.
- Petersen, T. A., Brown, L. D., Cook, F. A., Kaufman, S., and Oliver, J. E. (1984). Structure of the Riddleville Basin from COCORP Seismic Data and Implications for Reactivation Tectonics. *The Journal of Geology*, 92(3):261–271.
- Platt, J. P. and England, P. C. (1994). Convective removal of lithosphere beneath mountain belts; thermal and mechanical consequences. *American Journal of Science*, 294(3):307–336.
- Powell, C. M. and Williams, G. D. (1989). The Lewis Thrust/Rocky Mountain trench fault system in Northwest Montana, USA: an example of negative inversion tectonics? *Geological Society, London, Special Publications*, 44(1):223–234.
- Prijac, C., Doin, M., Gaulier, J., and Guillocheau, F. (2000). Subsidence of the Paris Basin and its bearing on the late Variscan lithosphere evolution: a comparison between Plate and Chablis models. *Tectonophysics*, 323(1-2):1–38.
- Prost, A. and Becq-Giraudon, J. (1989). Evidence for mid-Permian compressive tectonics in Western Europe supported by a comparison with the Alleghanian geodynamic evolution. *Tectonophysics*, 169(4):333–340.
- Pruvost, P. (1934). Bassin houiller de la Sarre et de la Lorraine. *Description Géologique et Gîtes Minéraux de France*, tome 3:174 pages.
- Pruvost, P. (1956). Orogenic saalic phase in France. *Zeitschrift der Deutschen Geologischen Gesellschaft*, 108(3):102–106.
- Rey, P., Vanderhaeghe, O., and Teyssier, C. (2001). Gravitational collapse of the continental crust: definition, regimes and modes. *Tectonophysics*, 342(3-4):435–449.
- Robin, C., Allemand, P., Burov, E., Doin, M. P., Guillocheau, F., Dromart, G., and Garcia, J.-P. (2003). Vertical movements of the Paris Basin (Triassic-Pleistocene): from 3D stratigraphic database to numerical models. *Geological Society, London, Special Publications*, 212(1):225–250.
- Rodrigues, R. d. S., Alves da Silva, F. C., and Venâncio, M. B. (2023). Oblique rifting along transfer zones: The structural evolution model revealed by physical modeling. *Journal of South American Earth Sciences*, 121:104153.
- Roure, F., Polino, R., and Nicolich, R. (1990). Early Neogene deformation beneath the Po plain: constraints on the post-collisional Alpine evolution. *Mémoires de la Société Géologique de France*, 156:309–322.
- Schäfer, A. (1989). Variscan molasse in the Saar-Nahe Basin (W-Germany), Upper Carboniferous and Lower Permian. *Geologische Rundschau*, 78(2):499–524.
- Schäfer, A. (2011). Tectonics and sedimentation in the continental strike-slip Saar-Nahe Basin (Carboniferous-Permian, West Germany). *Zeitschrift der Deutschen Gesellschaft für Geowissenschaften*, 162(2):127–155.
- Schäfer, A. and Korsch, R. (1998). Formation and sediment fill of the Saar-Nahe Basin (Permo-Carboniferous, Germany). *Zeitschrift der Deutschen Geologischen Gesellschaft*, 149(2):233–269.
- Schintgen, T. and Förster, A. (2013). Geology and basin structure of the Trier-Luxembourg Basin ? implications for the existence of a buried Rotliegend graben. *Zeitschrift der*

- Deutschen Gesellschaft für Geowissenschaften*, 164(4):615–637.
- Schlische, R. W. and Withjack, M. O. (2009). Origin of fault domains and fault-domain boundaries (transfer zones and accommodation zones) in extensional provinces: Result of random nucleation and self-organized fault growth. *Journal of Structural Geology*, 31(9):910–925.
- Schneider, J. and Romer, R. (2010). The Late Variscan molasses (Late Carboniferous to Late Permian) of the Saxo-Thuringian. In Linnemann, U. and Romer, R., editors, *Pre-Mesozoic Geology of Saxo-Thuringia: From the Cadomian Active Margin to the Variscan Orogen*, pages 323–346. Schweizerbart.
- Schneider, J. W., Lucas, S. G., Scholze, F., Voigt, S., Marchetti, L., Klein, H., Opluštil, S., Werneburg, R., Golubev, V. K., Barrick, J. E., Nemyrovska, T., Ronchi, A., Day, M. O., Silantiev, V. V., Rößler, R., Saber, H., Linnemann, U., Zharinova, V., and Shen, S.-Z. (2020). Late Paleozoic–early Mesozoic continental biostratigraphy — Links to the Standard Global Chronostratigraphic Scale. *Palaeoworld*, 29(2):186–238.
- Schwab, K. (1987). Compression and right-lateral strike-slip movement at the Southern Hunsrück Borderfault (South-west Germany). *Tectonophysics*, 137(1-4):115–126.
- Sharp, I. R., Gawthorpe, R. L., Armstrong, B., and Underhill, J. R. (2000). Propagation history and passive rotation of mesoscale normal faults: implications for synrift stratigraphic development. *Basin Research*, 12(3-4):285–305.
- Smith, R. B. and Bruhn, R. L. (1984). Intraplate extensional tectonics of the Eastern basin-Range: Inferences on structural style from seismic reflection data, regional tectonics, and thermal-mechanical models of brittle-ductile deformation. *Journal of Geophysical Research: Solid Earth*, 89(B7):5733–5762.
- Stein and Blundell, D. (1990). Geological inheritance and crystal dynamics of the northwest Scottish continental shelf. *Tectonophysics*, 173(1-4):455–467.
- Stollhofen, H. (1998). Facies architecture variations and seismogenic structures in the Carboniferous–Permian Saar–Nahe Basin (SW Germany): evidence for extension-related transfer fault activity. *Sedimentary Geology*, 119(1-2):47–83.
- Stollhofen, H. and Stanistreet, I. G. (1994). Interaction between bimodal volcanism, fluvial sedimentation and basin development in the Permo-Carboniferous Saar-Nahe Basin (south-west Germany). *Basin Research*, 6(4):245–267.
- Tari, G., Connors, C., Flinch, J., Granath, J., Pace, P., Sobornov, K., and Soto, J. I. (2023). Negative structural inversion: an overview. *Marine and Petroleum Geology*, 152:106223.
- Tari, G., Horváth, F., and Rumpel, J. (1992). Styles of extension in the Pannonian Basin. *Tectonophysics*, 208(1-3):203–219.
- Tavani, S., Carola, E., Granado, P., Quintà, A., and Muñoz, J. A. (2013). Transpressive inversion of a Mesozoic extensional forced fold system with an intermediate décollement level in the Basque-Cantabrian Basin (Spain). *Tectonics*, 32(2):146–158.
- Tavarnelli, E. (1999). Normal faults in thrust sheets: pre-orogenic extension, post-orogenic extension, or both? *Journal of Structural Geology*, 21(8-9):1011–1018.
- Van Hoorn, B. (1987). The south Celtic Sea/Bristol Channel Basin: origin, deformation and inversion history. *Tectonophysics*, 137(1-4):309–334.
- Velasco, M. S., Bennett, R. A., Johnson, R. A., and Hreinsdóttir, S. (2010). Subsurface fault geometries and crustal extension in the eastern Basin and Range Province, western U.S. *Tectonophysics*, 488(1-4):131–142.
- Voigt, S., Schindler, T., Tichomirowa, M., Käbner, A., Schneider, J. W., and Linnemann, U. (2022). First high-precision U–Pb age from the Pennsylvanian-Permian of the continental Saar–Nahe Basin, SW Germany. *International Journal of Earth Sciences*, 111(7):2129–2147.
- von Seckendorff, V., Arz, C., and Lorenz, V. (2004). Magmatism of the late Variscan intermontane Saar-Nahe Basin (Germany): a review. *Geological Society, London, Special Publications*, 223(1):361–391.
- Weber, K. (1995). The Saar-Nahe Basin. In *Pre-Permian Geology of Central and Eastern Europe*, pages 182–185. Springer Berlin Heidelberg, Berlin, Heidelberg.
- Williams, G. D., Powell, C. M., and Cooper, M. A. (1989). Geometry and kinematics of inversion tectonics. *Geological Society, London, Special Publications*, 44(1):3–15.
- Withjack, M. and Olson, J. (1990). Experimental Models of Extensional Forced Folds (1). *AAPG Bulletin*, 74:1038–1054.
- Žák, J., Svojtka, M., and Opluštil, S. (2018). Topographic inversion and changes in the sediment routing systems in the Variscan orogenic belt as revealed by detrital zircon and monazite U Pb geochronology in post-collisional continental basins. *Sedimentary Geology*, 377:63–81.
- Zeh, A. and Gerdes, A. (2010). Baltica- and Gondwana-derived sediments in the Mid-German Crystalline Rise (Central Europe): Implications for the closure of the Rheic ocean. *Gondwana Research*, 17(2-3):254–263.